[17,18]. Viral RNA in plasma was extracted and purified using the QIAamp Viral RNA Mini Kit (Qiagen, Valencia, California, USA). For quantitative analysis of the RNA, the TaqMan system (Applied Biosystems, Foster City, California, USA) was used with primers and probes targeting the SIVmac239 *gag* region. The viral RNA was amplified using TaqMan EZ RT-PCR Kit (Applied Biosystems) with primers. The RT-PCR product was quantitatively monitored by its fluorescent intensity with ABI7700 (Applied Biosystems). Plasma viral load, which was measured in duplicate, was calculated based on the standard curve of control RNA and RNA recovery rate. The limit of detection was approximately 500 RNA copies/ml.

Flow cytometric evaluation of cell surface antigen expression and absolute cell count

Lymphoid cells for flow cytometric analyses were prepared from intact thymuses, spleens, and lymph nodes. Mouse mAbs conjugated with either fluorescein isothiocyanate (FITC), phycoerythrin, phycoerythrin-Cy5, or peridinin chlorophyll protein (PerCP) were used in flow cytometric analyses to detect cellular expression of monkey CD3 (NF-18; BioSource International, Camarillo, California, USA), human CD4 (SK3; Becton Dickinson, San Jose, California, USA), and CD8 (SK1; Becton Dickinson). To determine absolute cell counts, samples of whole blood were analyzed following the addition of FITC-conjugated anti-CD3 (BioSource), phycoerythrin-conjugated anti-CD4 (Becton Dickinson), and PerCP-conjugated anti-CD8 mAbs (Becton Dickinson), as previously described [19].

Results

KD-247 concentrations and detection of anti-KD-247 antibodies in monkey plasma

Blood was drawn from monkeys before and after the administration of KD-247 and at necropsy (Fig. 1a). In the monkeys that were given antibody beginning 1 h (Cy-1 and Cy-2) or 1 day (Cy-3 and Cy-4) after challenge with SHIV-C2/1, concentrations of KD-247 peaked at 800–2000 μg/ml at 15 min after injection and were maintained at 200–500 μg/ml until the next administration (as evidenced in blood samples drawn before each administration and within 15 min of the injection) (Fig. 1b i and ii). The plasma concentrations of KD-247 in monkeys treated beginning 1 week after challenge with the virus (Cy-5 and Cy-6) did not remain constant. In particular, the KD-247 maintenance concentrations in Cy-6 after day 22 were below the limit of detection (2.5 μg/ml) of the assay (Fig. 1b iii).

Because KD-247 was repeatedly administered to the monkeys, we also considered the possibility of anti-KD-247 antibody production. Anti-KD-247 antibodies in monkey plasma (1 : 400 dilution) were measured using samples collected at necropsy. Binding activity indicated that the number of anti-KD-247 antibodies in Cy-6 was significantly higher than in the other monkeys (Fig. 2a). To clarify the sites of recognition of the anti-KD-247 antibodies in Cy-6, the binding activity of antibodies in Cy-6 plasma to other anti-HIV-1 antibodies was investigated. Rμ5.5 is a reshaped mAb that is equivalent to the entire KD-247 molecule except for antigen-binding sites [6,20], and Cβ1 is a chimeric mAb whose Fc region is equivalent to that of KD-247 [21]. These mAbs were used, as well as KD-247 coated for ELISA. The reaction of these mAbs with the monkey antibodies was detected by biotinylated KD-247 based on a double-antibody capture ELISA. The antibodies bound to KD-247 in Cy-6 plasma reacted with neither Rμ5.5 nor Cβ1 (Fig. 2b). Finally, we examined whether anti-KD-247 antibodies in Cy-6 plasma inhibit the binding of KD-247 to antigen peptides. Two KD-247-specific antigen peptides, SP13 and P20PATH (NNTRRRLSIGPGRA-FYARRN), derived from the V3 region of SHIV-C2/1, were coated on ELISA plates and reacted with KD-247 that had been incubated overnight at 4°C with Cy-6 plasma collected on day 0, day 7, or at necropsy. Binding of KD-247 to antigen peptides decreased by approximately 60% after reaction of mAb with Cy-6 plasma collected at necropsy (Fig. 2c). Antibody inhibition of the binding of KD-247 to antigen peptides strongly suggests that the plasma contained an antiidiotype antibody.

Suppression of plasma viral load and of $CD4^+$ T-cell loss in peripheral blood

The kinetics of plasma viral load in monkey plasma is shown in Fig. 3(a). The viral loads were suppressed in monkeys given KD-247 in comparison with those given control IgG. The complete protection previously reported with preadministration of KD-247 was not achieved in these postadministration trials [7]. The $CD4^+$ T-cell counts were maintained at higher levels in monkeys given KD-247 than in the control animals (Fig. 3b). The suppression of viral load and the maintenance effect of KD-247 on $CD4^+$ T cells were similar among the test groups. As each group had only two animals, between-group significant differences were not tested.

Maintenance of $CD4^+$ T cells in various lymphoid tissues

At 11–13 weeks after viral challenge, necropsies of the monkeys given KD-247 were performed and their lymphoid organs were evaluated. All the lymph nodes of the monkeys inoculated with pathogenic SHIV followed by control IgG were atrophied. In contrast, the lymph nodes of all monkeys given KD-247 maintained normal shape. Marked change was observed in the thymus (Fig. 4a); the thymuses of all monkeys given KD-247 were hypertrophic, whereas the thymuses of monkeys inoculated with SHIV alone, or given control IgG, were atrophied. No organ atrophy was observed in any of the

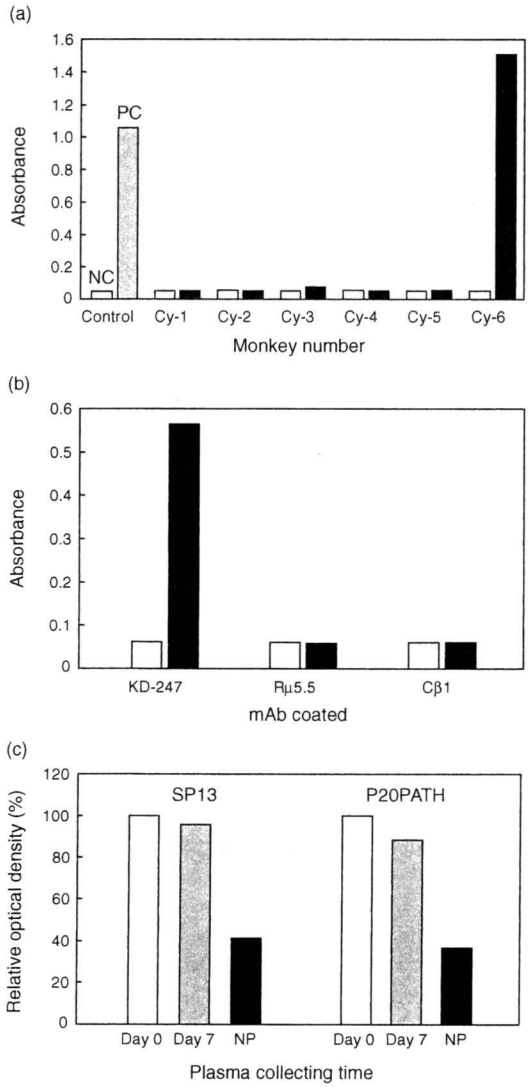

Fig. 2. Properties of anti-KD-247 antibodies in Cy-6 monkey plasma. (a) Anti-KD-247 activity of plasma in monkeys given KD-247. Open and closed bars indicate the binding activities of anti-KD-247 antibodies to KD-247 in monkey plasma collected at day 0 and necropsy, respectively. NC, negative control using the sample diluent; PC, positive control using a goat antibody to human IgG (200 ng/ml; ICN/Cappel, Aurora, Ohio, USA). (b) Binding of Cy-6 plasma to humanized and chimeric mAbs. Open and closed bars indicate binding activities of anti-KD-247 antibodies to KD-247 in monkey plasma collected on day 0 and at necropsy (day 88), respectively. (c) Inhibitory effect of Cy-6 plasma on the binding of KD-247 to antigen peptides SP13 (left) and P20PATH (right). The plasma samples collected on day 7 and at necropsy had been incubated with these peptides. Suppression of the binding of KD-247 to the peptides is shown as relative optical density (%) to the binding of KD-247 incubated with plasma collected on day 0. IgG, immunoglobulin G; NP, necropsy.

groups treated with KD-247. To determine the architecture of the lymph nodes, we examined tissue sections collected at necropsy. Germinal centers were not detected in the lymphoid tissue of monkeys treated with control IgG, but cell architecture was preserved in monkeys given KD-247 (Fig. 4b).

The T-cell subpopulation in the lymphoid tissues of the monkeys was analyzed by flow cytometry (Fig. 5). The $CD4^+$ T cells in the lymph nodes of both the IgG control monkeys (Cy-7 and Cy-8) were nearly depleted. In contrast, a normal level of $CD4^+CD8^-$ cells was maintained in the lymph nodes of all monkeys given KD-247. The $CD4^+CD8^-$ T-cell population values in the groups given KD-247 and control IgG were obviously higher and lower, respectively, than the values for the mean − 2 SD in naive control monkeys ($n = 15$). In the thymus, the absolute cell numbers of the monkeys given control IgG were low and could not be assessed for Cy-7 lymphocytes because of cell depletion. Thymic T-cell subpopulations were composed almost entirely of $CD4^+CD8^+$ double-positive cells (Cy-1 = 52%, Cy-2 = 74%, Cy-3 = 75%, Cy-4 = 76%, Cy-5 = 77%, Cy-6 = 75%, and Cy-8 = 71%; naive = 63 ± 15%). In the submandibular and mesenteric lymph nodes and spleen, administration of KD-247 rescued $CD4^+CD8^-$ cells independently of injection timing; this T-cell subset was not maintained in IgG controls.

Discussion

Since the development of HAART, the likelihood of progression to AIDS or death has been decreased if $CD4^+$ T-cell counts are properly maintained even when HIV-1 RNA concentrations in peripheral blood are high [22]. This finding suggests importance of maintaining $CD4^+$ T cells in the whole body for the control of HIV/AIDS. In this study, we confirmed that postinfection passive immunization of SHIV-infected monkeys with KD-247 fully rescued $CD4^+$ T-cell loss in various lymphoid tissues and yielded partial protection against increased plasma viral load and loss of $CD4^+$ T cells.

How, then, does postinfection immunization with KD-247 help maintain $CD4^+$ T cells in lymphoid tissues? Immunohistological alterations of the lymph nodes in HIV-infected patients represent a dynamic process, in which an initial florid follicular hyperplasia gives way ultimately to lymphocyte depletion [23]. There are several theories regarding the various direct or indirect mechanisms of $CD4^+$ lymphocyte depletion by HIV [24]. We previously reported that treatment with the humanized neutralizing antibody Rμ5.5 prevented HIV-1-induced atrophic changes in the medulla of engrafted thymic tissue in a thymus/liver-transplanted severe combined immunodeficient murine model [20]. The acute pathogenic SHIV-C2/1-derived clone virus KS661 resulted in increased thymic involution, atrophy, and the depletion of immature T cells, including $CD4^+CD8^+$ double-positive cells [25]. Infection with HIV-1, SIV, or

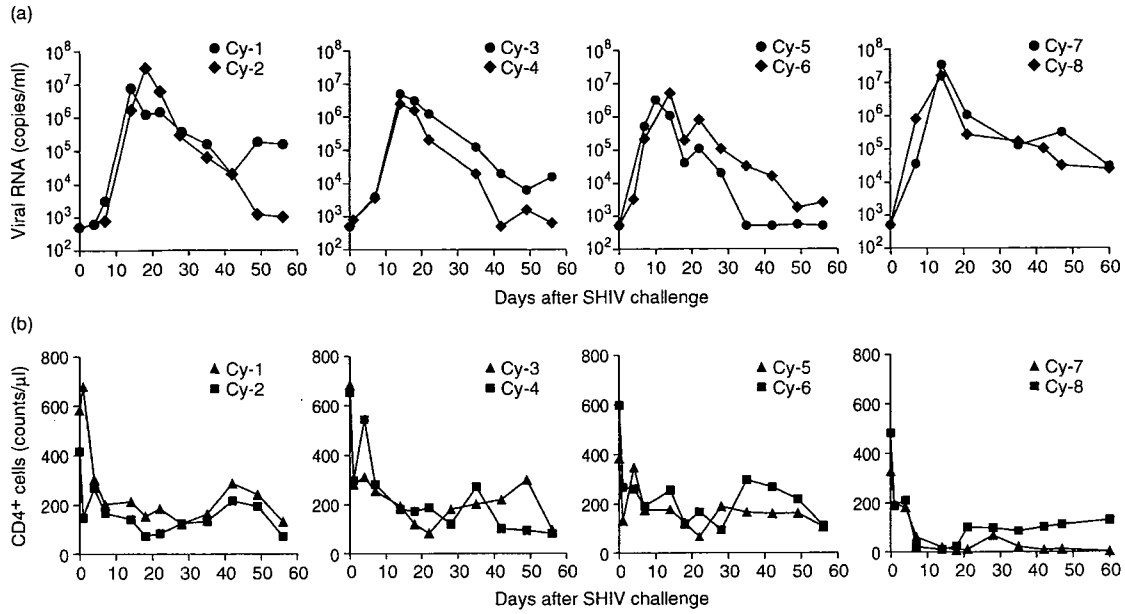

Fig. 3. Plasma viral loads and CD4$^+$ T-cell counts after viral challenge. Postchallenge plasma viral RNA copies and absolute CD4$^+$ T-cell counts in the peripheral blood were detected in the monkeys in each of four groups treated with KD-247 antibody or control IgG after infection as described in Fig. 1(a). (a) Kinetic changes in viral RNA copy numbers per ml of peripheral blood. (b) Kinetics of CD4$^+$ T-cell counts. IgG, immunoglobulin G; SHIV, simian/human immunodeficiency virus.

SHIV is associated with abnormalities in the number, size, and structure of germinal centers [26]. Progressive depletion of proliferating B cells and disruption of the follicular dendritic cell network in germinal centers within 20 days after SIV challenge have also been reported [27]. Although our study was limited by small group size (two monkeys/group), our data clearly show only minimal differences in CD4$^+$ T-cell levels between groups treated with KD-247 and the IgG control monkeys. The effects of KD-247 on CD4$^+$ T cells were more remarkable in lymph node than in peripheral blood compartments. Accumulation of apoptotic cells has been reported in both lymph nodes and thymus during the second week of highly pathogenic SHIV-C2/1 [17,28] and $SHIV_{DH12R}$ infections [29]. Given the smaller increase in CD4$^+$CD95$^+$ cell populations in peripheral blood mononuclear cells among monkeys that exhibited even partial protection from postchallenge SHIV-C2/1 with a suboptimal dose of KD-247 infusion in previous studies [7], KD-247 might protect against apoptosis of CD4$^+$ T cells in lymphoid tissues. Thus, in addition to neutralizing antibodies in animals receiving transfusions, passive transfer of KD-247 might help to maintain levels of CD4$^+$ T cells and to preserve the integrity of lymphoid structures, potentially leading to a less pathogenic course of disease progression. The roles played by the antibodies against HIV/AIDS could be clarified by further analyses of immunological function of monkeys treated with KD-247; areas of future research include viral components [30,31], lymphocyte activation [32,33], cytokine spectra [34], T-cell homeostasis [35,36], dendritic cell functions [37,38], Fc receptor interactions [39,40], and related functions.

Because preinfection experiments have shown that the concentration of KD-247 in plasma is important in protecting monkeys against viral infection [7], we also measured KD-247 concentrations in plasma samples. The postinfection effect of KD-247 against increased viral load and CD4$^+$ T-cell loss in peripheral blood were evaluated. Monkeys given KD-247 had lower plasma viral loads and less CD4$^+$ T-cell loss than did those treated with control IgG; however, as noted above, each group had only two animals and no statistical analysis was performed. These results in peripheral blood were not very pronounced compared with the phenomena observed in lymphoid organs. Complete protection, which was previously reported with preinfection administration of KD-247 [7], was not achieved in these postinfection trials. The times and values of viral load peaks were similar in all monkeys, but the increases in viral loads were delayed by administration of KD-247. Interestingly, the ability of KD-247 to suppress viral loads after they peaked did not depend on the timing of administration. In previous preinfection experiments with 45 mg/kg of KD-247, viral challenges were performed 1 day after KD-247 administration, and blood concentrations of KD-247 ranged from 700 to 800 μg/ml immediately before viral challenge in monkeys. Preadministration of these concentrations of KD-247 yielded complete protection against SHIV-C2/1 infection [7]. By contrast, in the current study, the monkeys given KD-247 1 h after

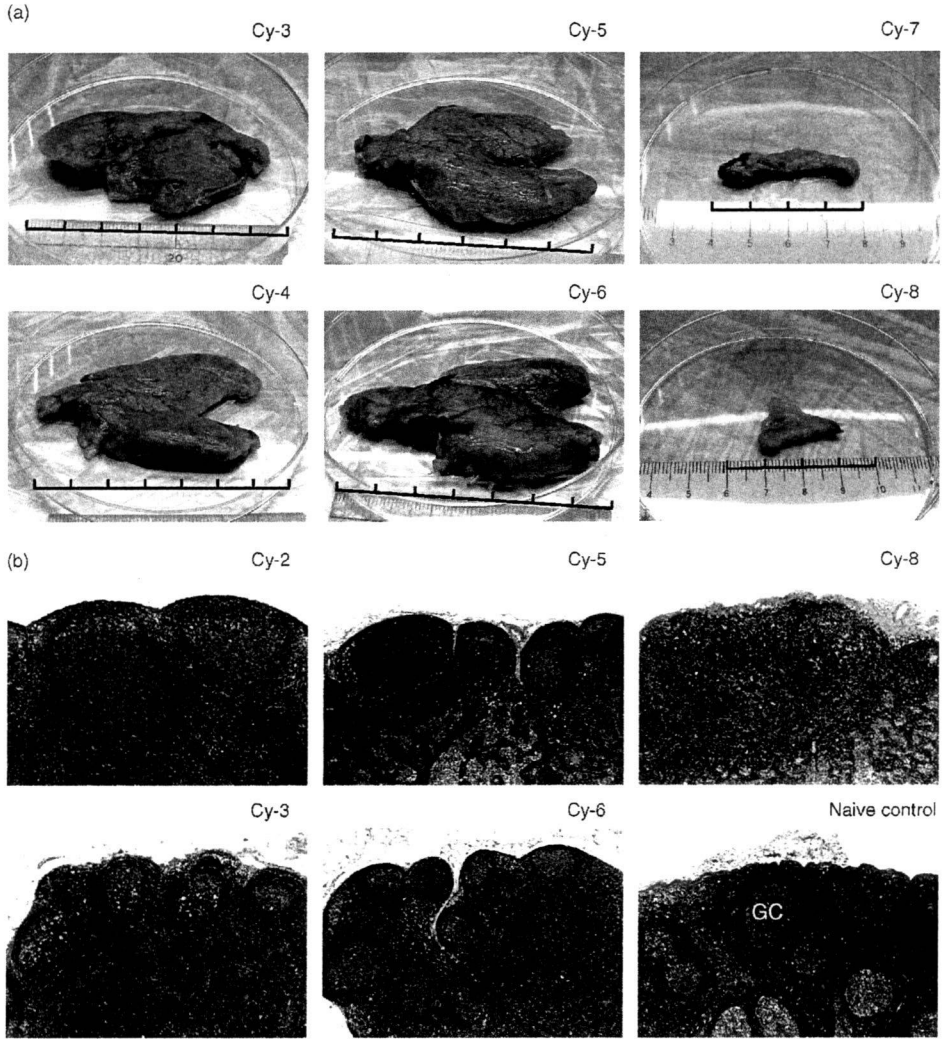

Fig. 4. Comparative postinfection protection against atrophic changes in lymphoid tissues. (a) Macroscopic images of thymus. Superimposed rulers indicate scales marked in centimeters. Although Cy-1, Cy-2, and naive control thymuses are not shown here, all thymuses of the monkeys given KD-247 were larger and those given control IgG were smaller than naive monkey thymuses. (b) Histological changes as postinfection effects of KD-247. Parts of the tissue blocks were preserved in 10% buffered formalin, embedded in paraffin. Tissue sections were stained with hematoxylin and eosin for conventional light microscopy (original magnification 18×). Mesenteric (Cy-2, Cy-5, and Cy-6), inguinal (Cy-3 and naive control), and submandibular (Cy-8) lymph nodes were photographed. Germinal centers, which are bright round areas (shown as GC in only the naive control), were maintained in the monkeys given KD-247, whereas the architecture of germinal centers in lymph node tissue from the control monkey given human normal IgG was not detected. GC, germinal centers; IgG, immunoglobulin G.

challenge with the virus became infected, even though the KD-247 concentrations 15 min after administration ranged from 1000 to 1300 μg/ml (Fig. 1b i). These KD-247 concentrations are considered sufficient to neutralize cell-free viruses that develop after the initial infection and/or are generated one after another following infection in peripheral blood. Therefore, the inability of the antibody administered 1 h after challenge to completely protect against the virus suggests that target cells were infected with the virus within 1 h. The previously reported results of time-dependence studies [10,11,41] of postinfection prophylaxis using SHIV are comparable with those obtained in the present study. The virus might not only infect target cells directly but also evade neutralizing antibody to produce infection in the cells of the peripheral blood and/or the lymphoid tissues [42,43]. Follicular dendritic cells could sustain HIV infection in the presence of neutralizing antibody [44]. Mucosal infection, such as vaginal challenge with SHIV, has been suggested to be a better in-vivo model to evaluate passive immunization [45,46]. The effects of antibodies in the lymph node compartment might be clearly observable using models of mucosal infection, as viruses harbored in lymph nodes after mucosal challenge later appeared in the peripheral blood compartment following systemic spread. Unexpectedly,

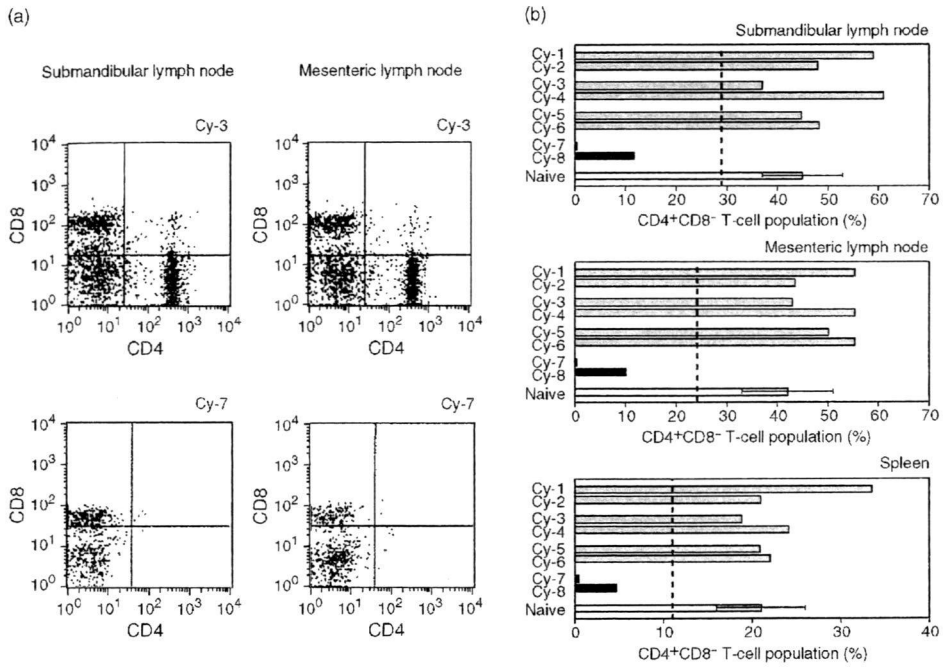

Fig. 5. Postinfection protection against tissue CD4$^+$ T-cell loss by passive transfer of KD-247 at various times after simian/human immunodeficiency virus C2/1 challenge. (a) Flow cytometric profiles of CD4$^+$ and CD8$^+$ T cells in the submandibular (left) and mesenteric (right) lymph nodes. Upper panels show maintenance of CD4$^+$ T cells in animal Cy-3 after passive transfer of KD-247. Lower panels show the loss of CD4$^+$ populations in the control IgG-treated animal Cy-7. (b) Postinfection protection of KD-247 against loss of CD4$^+$CD8$^-$ tissue lymphocytes. Tissue distributions of CD4$^+$CD8$^-$ T cells were determined in submandibular and mesenteric lymph nodes and spleen in animals of each group, as well as in those of naive control monkeys ($n = 15$). Bars indicate SD. Broken lines show the mean – 2 SD values of the naive control. IgG, immunoglobulin G.

the maintenance of CD4$^+$ T cells in the lymph nodes in Cy-6 were similar to those in the other monkeys given KD-247, although the mAb was eliminated from the plasma 3 weeks after viral challenge, once anti-KD-247 antibodies were elicited in this monkey. High plasma concentrations of KD-247 seem to be effective in preventing HIV-1 transmission. However, even if high concentrations are not maintained in the blood for a long time, KD-247 could rescue lymphoid CD4$^+$ T cells.

Passive immunization with mAbs has been shown to prevent a variety of diseases, although no mAb products are licensed for use for immunotherapy against HIV/AIDS [47]. In a passive immunization trial with humans, a cocktail of three mAbs was able to delay viral rebound following interruption of antiretroviral therapy [15]. However, differences in the pharmacokinetic profiles of constituent mAbs and cost-related issues of production might affect the development of neutralizing mAb cocktail drugs [47,48]. In contrast, KD-247 itself neutralizes primary isolates including chemokine (C–C motif) receptor 5 (CCR5)-tropic viruses with a matching narrow-neutralization sequence motif [6,7]. KD-247 is expected to be useful as a novel reagent for immune protection against HIV/AIDS, because the mAb might not only directly neutralize the virus but also maintain CD4$^+$ T cells in lymphoid tissues.

Acknowledgements

This work was supported by the 'Panel on AIDS' of the United States–Japan Cooperative Medical Science Program and the Health Science Foundation, Japan.

T. Murakami planned experiments, wrote the manuscript, and analyzed the laboratory data; M. Honda conducted the study, planned the experiments, and wrote the manuscript; Y. Eda planned and conducted the experiments; T. Nakasone, K. Someya, N. Yoshino, M. Kaizu, and Y. Izumi performed the animal experiments and analyzed the laboratory data; Y. Ami and H. Matsui performed the animal experiments and the pathological analyses; K. Shinohara managed the animal experiments; N. Yamamoto supervised the study.

Part of the information was presented at the 16th Annual Meeting of the Japanese Society for AIDS Research, 28–30 November 2002, Nagoya, Japan (abstract 249).

References

1. Douek DC, Kwong PD, Nabel GJ. **The rational design of an AIDS vaccine.** *Cell* 2006; **124**:677–681.
2. McMichael AJ. **HIV vaccines.** *Annu Rev Immunol* 2006; **24**: 227–255.

3. Haynes BF, Montefiori DC. **Aiming to induce broadly reactive neutralizing antibody responses with HIV-1 vaccine candidates.** *Expert Rev Vaccines* 2006; **5**:579–595.
4. Lin G, Nara PL. **Designing immunogens to elicit broadly neutralizing antibodies to the HIV-1 envelope glycoprotein.** *Curr HIV Res* 2007; **5**:514–541.
5. Emini EA, Schleif WA, Nunberg JH, Conley AJ, Eda Y, Tokiyoshi S, *et al.* **Prevention of HIV-1 infection in chimpanzees by gp120 V3 domain-specific monoclonal antibody.** *Nature* 1992; **355**:728–730.
6. Eda Y, Takizawa M, Murakami T, Maeda H, Kimachi K, Yonemura H, *et al.* **Sequential immunization with V3 peptides from primary human immunodeficiency virus type 1 produces cross-neutralizing antibodies against primary isolates with a matching narrow-neutralization sequence motif.** *J Virol* 2006; **80**: 5552–5562.
7. Eda Y, Murakami T, Ami Y, Nakasone T, Takizawa M, Someya K, *et al.* **Anti-V3 humanized antibody KD-247 effectively suppresses ex vivo generation of human immunodeficiency virus type 1 and affords sterile protection of monkeys against a heterologous simian/human immunodeficiency virus infection.** *J Virol* 2006; **80**:5563–5570.
8. Matsushita S, Takahama S, Shibata J, Kimura T, Shiosaki K, Eda Y, *et al.* **Ex vivo neutralization of HIV-1 quasi-species by a broadly reactive humanized monoclonal antibody KD-247.** *Hum Antibodies* 2005; **14**:81–88.
9. Haigwood NL, Montefiori DC, Sutton WF, McClure J, Watson AJ, Voss G, *et al.* **Passive immunotherapy in simian immunodeficiency virus-infected macaques accelerates the development of neutralizing antibodies.** *J Virol* 2004; **78**:5983–5995.
10. Nishimura Y, Igarashi T, Haigwood NL, Sadjadpour R, Donau OK, Buckler C, *et al.* **Transfer of neutralizing IgG to macaques 6 h but not 24 h after SHIV infection confers sterilizing protection: implications for HIV-1 vaccine development.** *Proc Natl Acad Sci U S A* 2003; **100**:15131–15136.
11. Ferrantelli F, Buckley KA, Rasmussen RA, Chalmers A, Wang T, Li P-L, *et al.* **Time dependence of protective postexposure prophylaxis with human monoclonal antibodies against pathogenic SHIV challenge in newborn macaques.** *Virology* 2007; **358**:69–78.
12. Ruprecht RM, Ferrantelli F, Kitabwalla M, Xu W, McClure HM. **Antibody protection: passive immunization of neonates against oral AIDS virus challenge.** *Vaccine* 2003; **21**:3370–3373.
13. Safrit JT, Ruprecht R, Ferrantelli F, Xu W, Kitabwalla M, Van Rompay K, *et al.*, Ghent IAS Working Group on HIV in Women and Children. **Immunoprophylaxis to prevent mother-to-child transmission of HIV-1.** *J Acquir Immune Defic Syndr* 2004; **35**:169–177.
14. Hammer SM, Saag MS, Schechter M, Montaner JSG, Schooley RT, Jacobsen DM, *et al.*, International AIDS Society-USA panel. **Treatment for adult HIV infection: 2006 recommendations of the International AIDS Society-USA panel.** *JAMA* 2006; **296**: 827–843.
15. Trkola A, Kuster H, Rusert P, Joos B, Fischer M, Leemann C, *et al.* **Delay of HIV-1 rebound after cessation of antiretroviral therapy through passive transfer of human neutralizing antibodies.** *Nat Med* 2005; **11**:615–622.
16. Shinohara K, Sakai K, Ando S, Ami Y, Yoshino N, Takahashi E, *et al.* **A highly pathogenic simian/human immunodeficiency virus with genetic changes in cynomolgus monkey.** *J Gen Virol* 1999; **80**:1231–1240.
17. Sasaki Y, Ami Y, Nakasone T, Shinohara K, Takahashi E, Ando S, *et al.* **Induction of CD95 ligand expression on T lymphocytes and B lymphocytes and its contribution to apoptosis of CD95-up-regulated CD4$^+$ T lymphocytes in macaques by infection with a pathogenic simian/human immunodeficiency virus.** *Clin Exp Immunol* 2000; **122**:381–389.
18. Kaizu M, Sato H, Ami Y, Izumi Y, Nakasone T, Tomita Y, *et al.* **Infection of macaques with an R5-tropic SHIV bearing a chimeric envelope carrying subtype E V3 loop among subtype B framework.** *Arch Virol* 2003; **148**:973–988.
19. Yoshino N, Ami Y, Terao K, Tashiro F, Honda M. **Upgrading of flow cytometric analysis for absolute counts, cytokines and other antigenic molecules of cynomolgus monkeys (*Macaca fascicularis*) by using antihuman cross-reactive antibodies.** *Exp Anim* 2000; **49**:97–110.
20. Okamoto Y, Eda Y, Ogura A, Shibata S, Amagai T, Katsura Y, *et al.* **In SCID-hu mice, passive transfer of a humanized antibody prevents infection and atrophic change of medulla in human thymic implant due to intravenous inoculation of primary HIV-1 isolate.** *J Immunol* 1998; **160**:69–76.
21. Matsushita S, Maeda H, Kimachi K, Eda Y, Maeda Y, Murakami T, *et al.* **Characterization of a mouse/human chimeric monoclonal antibody (Cβ1) to a principal neutralizing domain of the human immunodeficiency virus type 1 envelope protein.** *AIDS Res Hum Retroviruses* 1992; **8**:1107–1115.
22. Egger M, May M, Chêne G, Phillips AN, Ledergerber B, Dabis F, *et al.*, and the ART Cohort Collaboration. **Prognosis of HIV-1-infected patients starting highly active antiretroviral therapy: a collaborative analysis of prospective studies.** *Lancet* 2002; **360**:119–129.
23. Wood GS. **The immunohistology of lymph nodes in HIV infection: a review.** *Prog AIDS Pathol* 1990; **2**:25–32.
24. Cloyd MW, Chen JJY, Adeqboyega P, Wang L. **How does HIV cause depletion of CD4 lymphocytes? A mechanism involving virus signaling through its cellular receptors.** *Curr Mol Med* 2001; **1**:545–550.
25. Motohara M, Ibuki K, Miyake A, Fukazawa Y, Inaba K, Suzuki H, *et al.* **Impaired T-cell differentiation in the thymus at the early stages of acute pathogenic chimeric simian-human immunodeficiency virus (SHIV) infection in contrast to less pathogenic SHIV infection.** *Microbes Infect* 2006; **8**:1539–1549.
26. Margolin DH, Saunders EH, Bronfin B, de Rosa N, Axthelm MK, Goloubeva OG, *et al.* **Germinal center function in the spleen during simian HIV infection in rhesus monkeys.** *J Immunol* 2006; **177**:1108–1119.
27. Zhang Z-Q, Casimiro DR, Schleif WA, Chen M, Citron M, Davies M-E, *et al.* **Early depletion of proliferating B cells of germinal center in rapidly progressive simian immunodeficiency virus infection.** *Virology* 2007; **361**:455–464.
28. Yoshino N, Ryu T, Sugamata M, Ihara T, Ami Y, Shinohara K, *et al.* **Direct detection of apoptotic cells in peripheral blood from highly pathogenic SHIV-inoculated monkey.** *Biochem Biophys Res Commun* 2000; **268**:868–874.
29. Igarashi T, Brown CR, Byrum RA, Nishimura Y, Endo Y, Plishka RJ, *et al.* **Rapid and irreversible CD4$^+$ T-cell depletion induced by the highly pathogenic simian/human immunodeficiency virus SHIV$_{DH12R}$ is systemic and synchronous.** *J Virol* 2002; **76**:379–391.
30. Gratton S, Cheynier R, Dumaurier M-J, Oksenhendler E, Wain-Hobson S. **Highly restricted spread of HIV-1 and multiply infected cells within splenic germinal centers.** *Proc Natl Acad Sci U S A* 2000; **97**:14566–14571.
31. de Paiva GR, Laurent C, Godel A, da Silva NA Jr, March M, Delsol G, *et al.* **Discovery of human immunodeficiency virus infection by immunohistochemistry on lymph node biopsies from patients with unexplained follicular hyperplasia.** *Am J Surg Pathol* 2007; **31**:1534–1538.
32. Zamarchi R, Barelli A, Borri A, Petralia G, Ometto L, Masiero S, *et al.* **B cell activation in peripheral blood and lymph nodes during HIV infection.** *AIDS* 2002; **16**:1217–1226.
33. Biancotto A, Iglehart SJ, Vanpouille C, Condack CE, Lisco A, Ruecker E, *et al.* **HIV-1-induced activation of CD4$^+$ T cells creates new targets for HIV-1 infection in human lymphoid tissue ex vivo.** *Blood* 2008; **111**:699–704.
34. Biancotto A, Grivel J-C, Iglehart SJ, Vanpouille C, Lisco A, Sieg SF, *et al.* **Abnormal activation and cytokine spectra in lymph nodes of people chronically infected with HIV-1.** *Blood* 2007; **109**:4272–4279.
35. Nokta MA, Li X-D, Nichols J, Pou A, Asmuth D, Pollard RB. **Homeostasis of naive and memory T cell subpopulations in peripheral blood and lymphoid tissues in the context of human immunodeficiency virus infection.** *J Infect Dis* 2001; **183**:1336–1342.
36. Letvin NL, Mascola JR, Sun Y, Gorgone DA, Buzby AP, Xu L, *et al.* **Preserved CD4$^+$ central memory T cells and survival in vaccinated SIV-challenged monkeys.** *Science* 2006; **312**:1530–1533.
37. Taruishi M, Terashima K, Dewan Z, Dewan MZ, Yamamoto N, Ikeda S, *et al.* **Role of follicular dendritic cells in the early HIV-1 infection: in vitro model without specific antibody.** *Microbiol Immunol* 2004; **48**:693–702.

38. Turville SG, Aravantinou M, Stössel H, Romani N, Robbiani M. **Resolution of de novo HIV production and trafficking in immature dendritic cells.** *Nat Methods* 2008; **5**:75–85.
39. Forthal DN, Landucci G, Phan TB, Becerra J. **Interactions between natural killer cells and antibody Fc result in enhanced antibody neutralization of human immunodeficiency virus type 1.** *J Virol* 2005; **79**:2042–2049.
40. Wilflingseder D, Banki Z, Garcia E, Pruenster M, Pfister G, Muellauer B, *et al.* **IgG opsonization of HIV impedes provirus formation in and infection of dendritic cells and subsequent long-term transfer to T cells.** *J Immunol* 2007; **178**:7840–7848.
41. Foresman L, Jia F, Li Z, Wang C, Stephans EB, Sahni M, *et al.* **Neutralizing antibodies administered before, but not after, virulent SHIV prevent infection in macaques.** *AIDS Res Hum Retroviruses* 1998; **14**:1035–1043.
42. Chen JJ-Y, Huang JC, Shirtliff M, Briscoe E, Ali S, Cesani F, *et al.* **CD4 lymphocytes in the blood of HIV$^+$ individuals migrate rapidly to lymph nodes and bone marrow: support for homing theory of CD4 cell depletion.** *J Leukoc Biol* 2002; **72**:271–278.
43. Malaspina A, Moir S, Nickle DC, Donoghue ET, Ogwaro KM, Ehler LA, *et al.* **Human immunodeficiency virus type 1 bound to B cells: relationship to virus replicating in CD4$^+$ T cells and circulating in plasma.** *J Virol* 2002; **76**:8855–8863.
44. Heath SL, Tew JG, Tew JG, Szakal AK, Burton GF. **Follicular dendritic cells and human immunodeficiency virus infectivity.** *Nature* 1995; **377**:740–744.
45. Kahn JO, Walker BD. **Acute human immunodeficiency virus type 1 infection.** *N Engl J Med* 1998; **339**:33–39.
46. Mascola JR. **Passive transfer studies to elucidate the role of antibody-mediated protection against HIV-1.** *Vaccine* 2002; **20**:1922–1925.
47. Bansal GP. **A summary of the workshop on passive immunization using monoclonal antibodies for HIV/AIDS, held at the National Institute of Allergy and Infectious Diseases, Bethesda, 10 March 2006.** *Biologicals* 2007; **35**:367–371.
48. Joos B, Trkola A, Kuster H, Aceto L, Fischer M, Stiegler G, *et al.* **Long-term multiple-dose pharmacokinetics of human monoclonal antibodies (mAbs) against human immunodeficiency virus type 1 envelope gp120 (mAb 2G12) and gp41 (mAbs 4E10 and 2F5).** *Antimicrob Agents Chemother* 2006; **50**:1773–1779.

Follicular Dendritic Cells Activate HIV-1 Replication in Monocytes/Macrophages through a Juxtacrine Mechanism Mediated by P-Selectin Glycoprotein Ligand 1[1]

Kenji Ohba,*† Akihide Ryo,[2]* Md. Zahidunnabi Dewan,*†‡ Mayuko Nishi,* Toshio Naito,§ Xiaohua Qi,† Yoshio Inagaki,† Yoji Nagashima,¶ Yuetsu Tanaka,‖ Takashi Okamoto,# Kazuo Terashima,† and Naoki Yamamoto[2]*†

Follicular dendritic cells (FDCs) are located in the lymphoid follicles of secondary lymphoid tissues and play a pivotal role in the selection of memory B lymphocytes within the germinal center, a major site for HIV-1 infection. Germinal centers are composed of highly activated B cells, macrophages, CD4$^+$T cells, and FDCs. However, the physiological role of FDCs in HIV-1 replication remains largely unknown. We demonstrate in our current study that FDCs can efficiently activate HIV-1 replication in latently infected monocytic cells via an intercellular communication network mediated by the P-selectin/P-selectin glycoprotein ligand 1 (PSGL-1) interaction. Upon coculture with FDCs, HIV-1 replication was significantly induced in infected monocytic cell lines, primary monocytes, or macrophages. These cocultures were found to synergistically induce the expression of P-selectin in FDCs via NF-κB activation and its cognate receptor PSGL-1 in HIV-1-infected cells. Consistent with this observation, we find that this response is significantly blocked by antagonistic Abs against PSGL-1 and almost completely inhibited by PSGL-1 small interfering RNA. Moreover, a selective inhibitor for Syk, which is a downstream effector of PSGL-1, blocked HIV-1 replication in our cultures. We have thus elucidated a novel regulatory mechanism in which FDCs are a potent positive bystander that facilitates HIV-1 replication in adjacent infected monocytic cells via a juxtacrine signaling mechanism. *The Journal of Immunology,* **2009, 183: 524–532.**

The natural progression of HIV-1 infection consists of acute and chronic stages (1, 2). In the acute phase of viral infection, an initial peak level of plasma viremia appears within a couple of weeks of transmission. At this early time point in the course of infection, HIV-1 has disseminated to the lymphoid organs and viral reservoirs and latency have been established. The HIV-1 viral load stabilizes at a relatively low level after a period of acute viral infection, defined as the "set point," during which an immunological activation against HIV-1 is initiated. However, in tandem with seroconversion, HIV-1 production in reservoir or latently infected cells will eventually resume upon specific immunological responses such as host cytokine secretion or cell-mediated immune reactions (3–6).

Lymphoid organs have been proposed to function as a major reservoir for HIV-1 (7). During the course of HIV infection, T cells and macrophages in secondary lymphoid organs also become major reservoir cells for HIV-1 (8). Several in vitro studies have now identified potentially stable reservoirs of inducible latently infected CD4$^+$ cells carrying an integrated form of the viral genome (7–9). In addition to CD4$^+$ T cells, monocytes are thought to be major reservoirs for HIV-1 in vivo, since a number of blood monocytes are maintained in HIV-1-infected patients even during the late disease stages when T cells can be practically undetectable (10, 11). These observations suggest that infected CD4$^+$ T cells and macrophages provide sites as a stable reservoir and producer of HIV-1, causing the persistent production of progeny virus in lymphoid organs. However, it has not been well investigated how these reservoir cells can maintain sufficient levels of viral replication that will retain a sufficient viral load during the long course of this disease.

It is generally believed that the central point in the immune system is the lymphoid organs and germinal centers (GCs)[3] where several immune cell types are localized, although these circulate throughout the whole body (12–14). The GCs of secondary lymphoid tissues are composed of B cells, CD4$^+$ T cells, macrophages, and follicular dendritic cells (FDCs) (15–17). FDCs are characterized by the expression of CD21, CD35, CD40, and specific cell surface adhesion molecules including ICAM-1, VCAM-1, and the surface dendritic cell (DC) markers DC-SIGN and DRC-1 (16, 18–21). The FDCs play an important role in the

*AIDS Research Center, National Institute of Infectious Diseases, Toyama, Shinjyuku-ku, Tokyo, Japan; †Department of Molecular Virology, Graduate School of Medicine, Tokyo Medical and Dental University, Yushima, Bunkyo-ku, Tokyo, Japan; ‡Department of Pathology, New York University School of Medicine, New York, NY 10016; §Department of General Medicine, Juntendo University School of Medicine, Hongo, Bunkyo-ku, Tokyo, Japan; ¶Department of Pathology, Graduate School of Medicine, Yokohama City University, Fukuura, Kanazawa-ku, Kanagawa, Japan; ‖Department of Immunology, Graduate School of Medicine, University of the Ryukyus, Uehara, Okinawa, Japan; and #Department of Molecular and Cellular Biology, Nagoya City University Graduate School of Medical Sciences, Kawasumi, Mizuho-cho, Mizuho-ku, Nagoya, Aichi, Japan

Received for publication February 3, 2009. Accepted for publication April 25, 2009.

The costs of publication of this article were defrayed in part by the payment of page charges. This article must therefore be hereby marked *advertisement* in accordance with 18 U.S.C. Section 1734 solely to indicate this fact.

[1] This work was supported in part by grants from the Japanese Ministries of Education, Culture, Sports, Science and Technology (20390136, 13226027, 14406009, and 1941075) Health, Labour and Welfare (H18-005) and Human Health Science (H19-001) to N.Y. and A.R.

[2] Address correspondence and reprint requests to Dr. Akihide Ryo and Dr. Naoki Yamamoto, AIDS Research Center, National Institute of Infectious Diseases, 1-23-1 Toyama, Shinjyuku-ku, Tokyo 162-8640, Japan. E-mail addresses: aryo@nih.go.jp and nyama@nih.go.jp

[3] Abbreviations used in this paper: GC, germinal center; FDC, follicular dendritic cell; DC, dendritic cell; PSGL-1, P-selectin glycoprotein ligand 1; Syk, spleen tyrosine kinase; LTR, long terminal repeat; MOI, multiplicity of infection; siRNA, small interfering RNA.

www.jimmunol.org/cgi/doi/10.4049/jimmunol.0900371

immune response by interacting with $CD4^+$ T or B cells and in organization of the follicular structure.

In HIV infection, human FDCs can capture and retain infectious HIV particles in a stable manner on their cell surfaces for several months or even years via Fc receptors or other molecules (22–25). Unlike conventional DCs, FDCs are not themselves infected with HIV despite expression of chemokine receptors and DC-SIGN (24). Furthermore, active HIV infection is largely confined to sites surrounding the FDCs (24), suggesting that this microenvironment is highly conducive to infection with this virus. FDCs have also been shown to transmit signals to the GC microenvironment which also appears to increase HIV infection and replication (24, 25). Our previous study showed that FDCs stimulated virus production in MOLT-4 T cells preexposed to HIV-1(23). Very recently, Thacker et al. (26) also reported that FDCs contributed to virus replication in $CD4^+$ T cells infected with HIV-1 obtained from peripheral blood and GCs by increasing viral transcription mediated by TNF-α upon coculture. However, the role of FDCs in HIV-infected monocytes/macrophages is largely unknown.

We here report that FDCs can activate HIV-1 production in surrounding infected monocytes or macrophages via a cell-cell interaction with a clear mechanistic distinction from $CD4^+$ T cells reported by Thacker et al. (26). This enhancement in monocytic cells was found to be mediated mainly by an association between P-selectin on FDCs, acting as a ligand, and P-selectin glycoprotein ligand 1 (PSGL-1), the cognate receptor, on HIV-1-infected cells. Furthermore, we delineate the biological significance of the PSGL-1/spleen tyrosine kinase (Syk) pathway in the FDCs-mediated switch to induce HIV-1 replication. Our current findings thus shed new light on mechanisms involved in the HIV replication pathway that are mediated through intercellular communication and provide clues for the design of future novel therapeutic interventions against AIDS and related disorders.

Materials and Methods

Cell culture and reagents

Several FDC lines were established from fresh human palatine tonsils and maintained as described previously (23). Briefly, FDCs were isolated from fresh palatine tonsils surgically removed. Tonsils were cut into pieces in the thickness of 2–3 mm and then digested for 15 min at 37°C with collagenase (type I; Wako). Following rinsing with RPMI 1640 by centrifugation at 400 × *g* for 7 min, cells were filtered through at 70-μm nylon mesh and overlaid on a 1.25, 2.5, and 5% continuous BSA gradient at 1 × *g* for 2 h. The lowest fraction with a higher density fraction was resuspended and cultured in RPMI 1640 medium with 10% FCS. Cell clusters in the lowest fraction included cells positive for DRC-1, a specific maker of FDCs. One week after the culture, adherent spindle-shaped FDCs appeared from the cell clusters after having released lymphoid cells and spontaneously proliferated without additional cytokines or growth factors. The character of FDCs was checked with expression of FDCs makers such as CAN-42, S-100α, CD54, DC-SIGN, and CXCR4 on its surface. After culturing along more than 2 wk, FDCs were stocked in −80°C before use. PBMCs were separated from three healthy donors in accordance with the guidelines of the ethics committee of Tokyo Medical and Dental University. PBMCs were cultured in RPMI 1640 containing 10% FBS at 37°C in 5% CO_2. Primary monocytes were obtained from three healthy donors with Rosette Sep (StemCell Technologies) according to the manufacturer's instructions. Primary macrophages were differentiated from monocytes by culturing in RPMI 1640 containing 10% AB serum (Sigma-Aldrich) and 20 ng/ml M-CSF (R&D Systems) for 7 days. HIV-1 chronically infected monocytic cell line U1 cells (27) were cultured in RPMI 1640 supplemented with 10% FBS (Invitrogen Life Technologies). Coculturing and Transwell assays were performed using 1×10^5 HIV-infected cell lines or 2×10^5 primary cells with 1×10^4 FDCs. For the FDC supernatant assay, filtered (0.2 μm) supernatants from FDC cultures were collected and added to HIV-1-infected cells at a 1:4 volume supernatant:total volume of fluid ratio. In the cell fixation assay, FDCs incubated with 3% paraformaldehyde in PBS for 2 h were washed three times with PBS and then twice with RPMI 1640 before coculturing.

Virus preparation and infection

HIV-$1_{JR\text{-}FL}$ or HIV-$1_{NL4\text{-}3}$ viruses were generated by transfection of the pJR-FL or pNL4-3 construct in 293T cells, respectively. Virus preparations were passed through a 0.4-μm filter and titrated using a conventional method as described previously (28). For the HIV-1 infection of primary cells, PBMCs were infected with HIV-$1_{JR\text{-}FL}$ for 24 h following stimulation with PHA-P (3 μg/ml) for 3 days. To adjust the culture condition for monocytes/macrophages with that for PBMCs, monocytes or macrophages were also infected with HIV-$1_{JR\text{-}FL}$ for 24 h following stimulation with PHA-P (3 μg/ml) for 3 days. All primary cell cultures were maintained in the absence of IL-2. Jurkat or FDCs were infected with HIV-$1_{NL\text{-}4\text{-}3}$ (multiplicity of infection (MOI) = 0.05) for 1, 3, or 5 days.

Antibodies

Polyclonal Abs raised against phospho-p65 (Ser^{536}), phospho-Syk (Tyr^{352}), phospho-IκBα (Ser^{32}), and unmodified Syk were purchased from Cell Signaling Technology. Anti-p65 polyclonal, actin, and PSGL-1 (KPL1) mAb were purchased from Santa Cruz Biotechnology. Anti-α-tubulin mAb was purchased from Sigma-Aldrich. Neutralizing Abs targeting PSGL-1 or ICAM-1 were purchased from R&D Systems. Anti-HIV-1 p24 mAb (2C2; mouse IgG1) was produced by Y. Tanaka (University of Ryukyus, Okinawa, Japan).

Isolation of total RNA from cells and quantitative RT-PCR

U1 cells and FDCs were harvested after coculturing and washed three times with PBS. Total RNA was then extracted using Isogen (Nippongene) according to the manufacturer's instructions. RNA (1 μg) was reverse transcribed using Superscript III (Invitrogen) before semiquantitative RT-PCR, and quantitative RT-PCR was performed using a SYBER Green One-step Real-time PCR kit (Invitrogen) with mRNA-specific primer pairs. Analyzed genes and corresponding primers are listed in supplemental Table I.[4]

Neutralization assay

HIV-1-infected cells were pretreated with neutralizing Abs (anti-PSGL-1, anti-ICAM-1, or control mouse IgG) for 2 h before and during coculturing. Optimal concentrations were determined by the IC_{50} values in accordance with the manufacturer's instructions. Culture supernatants were collected after 3 days and subjected to measurement of HIV-1 p24.

Chemicals and inhibitory assays

BAY11-7082 and JNK inhibitor II were purchased from Merck. The Syk-specific inhibitor ER-27319 (29, 30) was purchased from Sigma-Aldrich. Cells were pretreated with 30 μM ER-27319, 1 μM JNK inhibitor II, 1–2 μM BAY11-7082, or DMSO (Sigma-Aldrich) for 2 h. The inhibitor treated/untreated cells were then cocultured with FDCs in the presence of Syk or NF-κB inhibitor. In small interfering RNA (siRNA) experiments, U1 cells were transfected with control or PSGL-1 siRNA (Santa Cruz Biotechnology) by Nucleofector (Amaxa) and then cocultured with FDCs. Lysates and supernatants were collected from these cultures after 3 days for measurement of p24 and Western blotting analysis.

Flow cytometry

Cells were washed twice with staining buffer (3% FBS and 0.09% NaN_3/PBS) and then stained with PSGL-1-RP-E (BD Biosciences) for 30 min on ice. Cells were then washed twice and processed for flow cytometry.

Measurement of HIV-1 p24

Cell culture supernatants were collected after centrifugation at 4000 rpm for 5 min at 4°C and then processed for measurement of HIV-1 p24 by using Lumipulse (Fujirebio) according to the manufacturer's instructions. Assays were performed in triplicate.

Results

FDCs activate HIV-1 production in adjacent HIV-1-infected monocytic cells

To address whether FDCs can also activate HIV-1 replication in the surrounding infected monocytes/macrophages as an effective bystander or stimulator, several primary FDCs were established from fresh palatine tonsils of three healthy human donors (23).

[4] The online version of this article contains supplemental material.

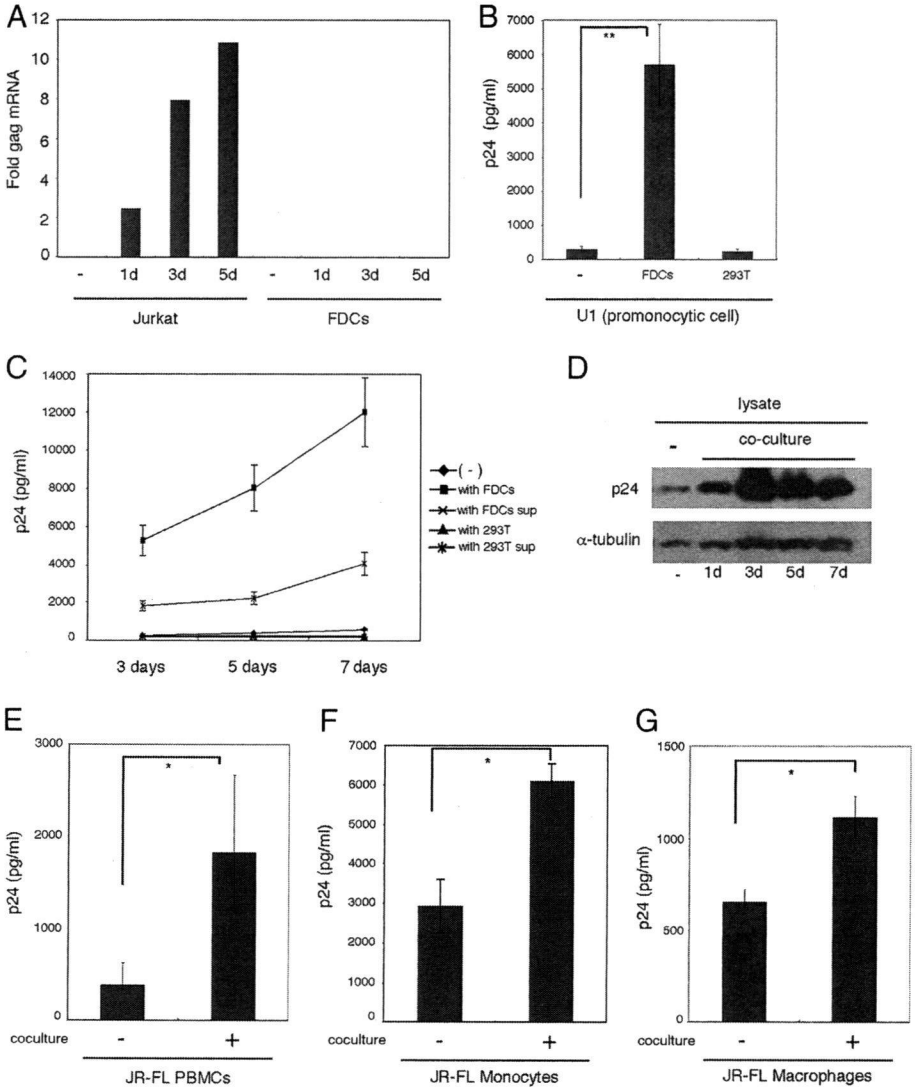

FIGURE 1. FDCs activate HIV-1 production in adjacent HIV-1-infected cells. *A*, Jurkat or FDCs were infected with HIV-1_{NL-4-3} (MOI = 0.05) for 1, 3, or 5 days. Cells were collected and then lysed for the separation of total RNA. Total RNA were treated with DNase I followed by quantitative RT-PCR with specific primer sets for either HIV-1 Gag or G3PDH. The data shown are the fold inductions normalized by G3PDH. *B*, U1 cells (1×10^5 cells/well) were cultured alone or in coculture with either FDCs or 293T cells (1×10^4 cells/well) for 3 days. Cell supernatants were then collected and assayed for measurement of p24. *C*, p24 levels in culture supernatants were monitored at 3, 5, and 7 days. *D*, p24 levels in lysates were monitored at 1, 3, 5, and 7 days by Western blot. *E*, PBMCs separated from a healthy donor were cultured with 3 μg/ml PHA for 3 days followed by infection with HIV-1_{JR-FL} (MOI = 0.05) for 24 h. The PBMCs (2×10^5 cells/well) were then cocultured with FDCs (1×10^4 cells/well) in the absence of IL-2 for 14 days. Culture supernatants were then assayed for measurement of p24. *F*, Monocytes separated from a healthy donor were cultured with 3 μg/ml PHA for 3 days followed by infection with HIV-1_{JR-FL} (MOI = 0.05) for 24 h. The monocytes (1×10^5 cells/well) were then cocultured with FDCs (1×10^4 cells/well) for 14 days. *G*, Primary differentiated macrophages were cultured with 3 μg/ml PHA for 3 days followed by infection with HIV-1_{JR-FL} (MOI = 0.05) for 24 h. The macrophages (1×10^5 cells/well) were then cocultured with FDCs (1×10^4 cells/well) for 7 days. Culture supernatants were then assayed for measurement of p24. The data shown in *B* are the average $\pm$ SD of at least three independent experiments. The data presented in *E–G* were obtained using samples of three donors (*, $p \leq 0.05$ and **, $p \leq 0.01$ by the Student *t* test).

Since each of these established cell lines was very similar in nature, exhibiting typical properties of FDCs (positive for CAN-42, S-100α, CD54, DC-SIGN, and CXCR4; morphological character such as spine-like spiculae and intercellular gap junction), the FDC 1 line was mainly used in subsequent experiments. FDCs themselves were not productively infected with HIV-1 (Fig. 1*A*), consistent with previous reports (22–25).

Initially, the FDCs were cocultured with chronically HIV-1-infected monocytic cell line U1 to examine whether they had the ability to activate HIV-1 replication. After 3 days of growth, HIV-1 production was analyzed for HIV-1 p24. The results showed that coculturing with FDCs significantly induced HIV-1 replication in the two infected cell types tested, whereas no such induction was observed when the U1 cells were cultured with 293T cells (Fig. 1*B*). A parallel kinetic study further demonstrated that the p24 levels in supernatants and lysates were increased in a time-dependent manner in U1 cells grown under these coculture conditions (Fig. 1, *C* and *D*). To address whether this trend occurred also in primary cells, FDCs were cocultured with PBMCs from healthy donors after infection with R5 (HIV-1_{JR-FL}) virus. As shown in Fig. 1*E*, the virus production was considerably augmented in coculture with FDCs. Furthermore, parallel experiments revealed that the virus production in monocytes or macrophages purified from PBMCs was also increased by coculturing with

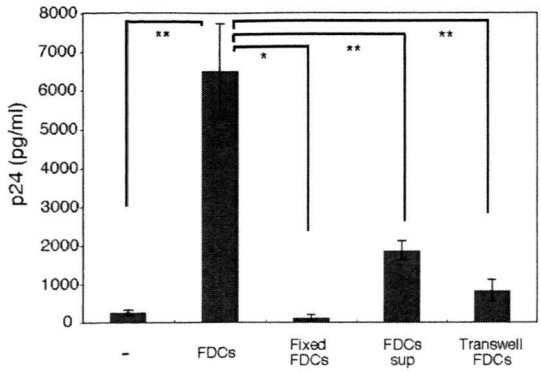

FIGURE 2. The enhancement of HIV-1 production by FDCs requires direct cell-cell interactions. U1 cells (1×10^5 cells/well) were cocultured with regular or paraformaldehyde-fixed FDCs (1×10^4 cells/well), cultured separately with FDCs on Transwell plates, or grown in medium supplemented with FDC culture supernatant at a 1:4 ratio of volume supernatant:total volume of fluid. Cell supernatants were collected after 3 days and assayed for measurement of p24. The data shown are the average ± SD of two independent experiments (*, $p \leq 0.05$ and **, $p \leq 0.01$ by the Student t test).

FDCs (Fig. 1, *F* and *G*). These data thus strongly indicate that FDCs can indeed activate viral replication monocytes/macrophages infected with HIV-1.

The enhancement of HIV-1 production by FDCs requires direct cell-cell interactions

To investigate whether this stimulation by FDCs was achieved by direct cell-cell interaction or soluble factors, we used two different cell culture methods for FDCs and U1 cells as follows: 1) FDCs were separately cultured with U1 cells using Transwells and 2) U1 cells were grown in culture medium supplemented with FDC supernatant. Although both culture systems could partially induce HIV-1 replication in U1 cells, these effects were ~20–30% of the full induction of those observed following coculture with FDCs (Fig. 2). This suggested that direct cell-cell interactions might be required for the full induction of HIV-1 replication in monocytic cells, although certain soluble factors may also activate HIV-1 replication to a lesser degree. Furthermore, the fixation of FDCs with paraformaldehyde before coculture completely abrogated the induction of HIV-1 replication in U1 cells, suggesting a requirement for bioactive cell surface molecules in this response.

Taken together, these data indicate that direct interactions via cell surface bioactive molecules are important to fully stimulate HIV-1 replication in monocytic U1 cells by FDCs.

Activation of NF-κB in both FDCs and HIV-1-infected cells following coculture

Our initial analysis demonstrated that FDCs can enhance HIV-1 replication in infected cells via cell-cell interaction. We thus examined whether this induction is initiated by the activation of the HIV-1 long-terminal repeat sequence (LTR). Quantitative and semiquantitative RT-PCR analyses revealed that the levels of HIV-1 mRNA were increased in U1 cells in tandem with increased supernatant p24 levels under coculture conditions with FDCs (Fig. 3, *A* and *B*).

HIV-1 replication has been shown to be regulated by host transcription factors such as NF-κB, NF-AT, Sp1, and AP-1 that are

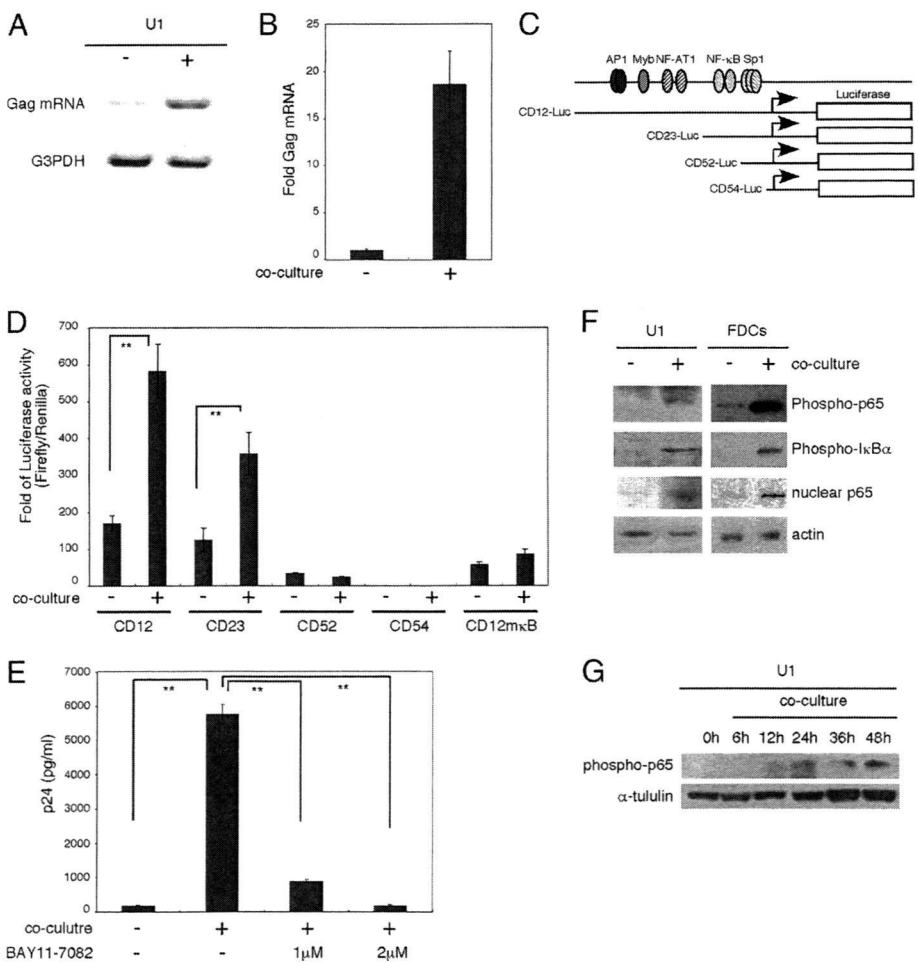

FIGURE 3. Activation of NF-κB in both FDCs and HIV-1-infected cells. *A* and *B*, U1 cells (1×10^5 cells/well) were cocultured with FDCs (1×10^4 cells/well) for 5 days and the mRNA levels for the indicated genes were measured by RT-PCR (*A*) or quantitative RT-PCR (*B*). *C*, Schematic representation of HIV-1 LTR-derived luciferase reporter constructs. *D*, U1 cells (1×10^5 cells/well) were initially transfected with the indicated reporter constructs and then cocultured with FDCs (1×10^4 cells/well) for 48 h, which was followed by a gene reporter assay. *E*, U1 cells (1×10^5 cells/well) were pretreated with the indicated concentrations of BAY 11-7082 for 2 h and then cocultured with FDCs (1×10^4 cells/well) for 3 days in the presence of the same concentration of BAY 11-7082. Cell supernatants were then collected and assayed for measurement of p24. *F*, U1 cells (1×10^5 cells/well) were cocultured with FDCs (1×10^4 cells/well) for 3 days and both cell types were collected and subjected to immunoblotting analysis for phospho-p65 (Ser^{536}), phospho-IκBα (Ser^{32}), p65, or actin. *G*, U1 cells (1×10^5 cells/well) were cocultured with FDCs (1×10^4 cells/well) and collected at the indicated time points. Cell lysates were subjected to immunoblot analysis using either phospho-p65 (Ser^{536}) or α-tubulin Abs. The data shown are the average ± SD of three independent experiments (*, $p \leq 0.05$ and **, $p \leq 0.01$ by the Student t test).

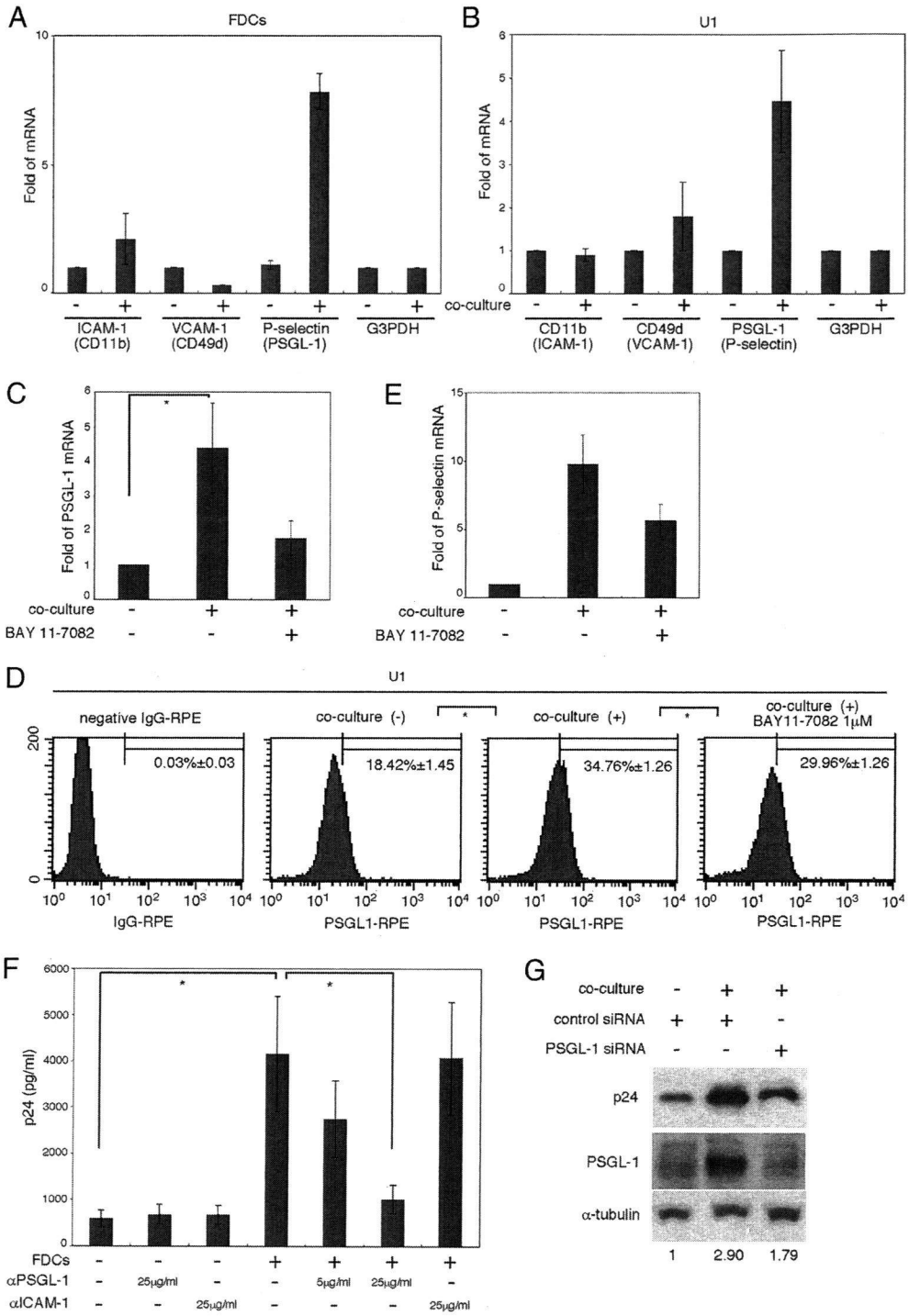

FIGURE 4. Involvement of P-selectin/PSGL-1 in reactivation of HIV-1 replication by FDC. *A* and *B*, U1 cells (1×10^5 cells/well) were cocultured with FDCs (1×10^4 cells/well) for 3 days. The mRNA levels of the indicated genes were then measured by quantitative RT-PCR. Labels inside parentheses indicate counterpart ligand or receptor molecules. *C–E*, U1 cells (1×10^5 cells/well) were cocultured with FDCs (1×10^4 cells/well) in the presence of BAY 11-7082 (1 μM) for 3 days and the levels of PSGL-1 in these cells were then analyzed by quantitative RT-PCR (*C*). Cell surface PSGL-1 was analyzed by flow cytometry using an anti-PSGL-1 Ab (*D*). M1 denotes the range of positive cell populations. *E*, P-selectin expression in FDCs analyzed by quantitative RT-PCR. *F*, U1 cells (1×10^5 cells/well) were untreated or pretreated with either PSGL-1 or ICAM-1 Ab for 1 h. Cells were then cocultured with FDCs (1×10^4 cells/well) for 3 days followed by measurement of p24. *G*, U1 cells (1×10^5 cells/well) were transduced with either control or PSGL-1 siRNA (final 6 nM) by Nucleofector according to the manufacturer's instructions. Cells were then cocultured with FDCs (1×10^4 cells/well) for 3 days followed by Western blot analysis with the indicated Abs. Numerical values below the blots indicate p24 signal intensities normalized by α-tubulin intensity derived by densitometry. The data shown are the average $\pm$ SD of three independent experiments (*, $p \leq 0.05$ and **, $p \leq 0.01$ by the Student t test).

recruited and bind directly to the HIV-1 LTR (31–33). To determine the identity of the *cis*-regulatory element(s) within the HIV-1 LTR that are the targets of FDC-mediated transcriptional activation, we examined various 5′-deletion mutants of these region as described in Fig. 3*C* (34). Coculturing of U1 cells with FDCs resulted in the activation of CD12 and CD23 reporter constructs

that harbor a NF-κB-binding sequence. However, the CD52 and CD54 constructs lacking this NF-κB consensus site were not activated, suggesting the involvement of NF-κB in the HIV-1 replication response (Fig. 3*D*). Consistent with this notion, the reporter construct CD12 that contains a site-directed mutation within the NF-κB binding site, CD12mκB, was not responsive to FDC stimulation. These results together indicate that the stimulation of HIV-1 in infected cells by FDCs is mediated via the activation of the HIV-1 LTR via NF-κB.

To further address this in terms of biological function, cells were treated with the NF-κB inhibitor BAY 11-7082 to further delineate the role of NF-κB in FDC-mediated HIV-1 replication. Treatment with BAY 11-7082 significantly suppressed HIV-1 production from U1 cells, even when growing in coculture with FDCs (Fig. 3*E*), although the viability of both cell types was not significantly affected by this exposure (data not shown). Taken together, our data thus indicate that intercellular communication pathways triggered by FDCs can promote and augment HIV-1 production in infected cells via NF-κB activation.

We next investigated whether NF-κB is in fact activated in FDCs as well as in U1 cells under coculture conditions. Consistent with our above gene reporter data, NF-κB activation was confirmed in U1 cells as revealed by the phosphorylation status of NF-κB p65 and IκBα (Fig. 3*F*). Interestingly, parallel experiments showed NF-κB activation in FDCs also in our coculture system, as revealed by immunoblotting with phospho-specific Abs (Fig. 3*F*). Furthermore, fractionation analysis demonstrated that the nuclear p65 (RelA) levels were significantly enhanced in both U1 and FDCs, indicating the nuclear accumulation of activated NF-κB (Fig. 3*F*). Parallel kinetic analysis revealed that NF-κB activation in U1 cells was initiated at 12 h and persisted for at least 48 h (Fig. 3*G*). These findings thus support our contention that cell-cell interactions between FDCs and U1 cells results in the constitutive activation of NF-κB in both cell types and that this is likely to be involved in the amplification of HIV-1 replication signals.

FDCs activate HIV-1 production via a P-selectin-PSGL-1 interaction

We were prompted to examine whether NF-κB up-regulates a specific cell surface ligand and its cognate receptor in FDCs and HIV-1-infected monocytic cells, eventually contributing to the amplification of HIV-1 replication signals via NF-κB activation. To this end, we examined the expression of different cell surface ligands and their cognate receptors which are known to be regulated by NF-κB. We chose three ligand/receptor combinations based upon a database search, ICAM-1/CD11b, VCAM-1/CD49d, and P-selectin/PSGL-1, and the expression of these molecules was analyzed by quantitative RT-PCR. Although the mRNA levels of ICAM-1 and VCAM-1 were not significantly altered upon stimulation, transcripts for P-selectin (CD62P/SLBP) were dramatically increased in FDCs (Fig. 4*A*). Interestingly, transcripts for the cognate receptor for P-selectin, PSGL-1, were found to be significantly up-regulated in U1 cells grown in coculture with the FDCs (Fig. 4*B*), but this was not the case for the CD11b and CD49d receptors. Quantitative RT-PCR and FACS analysis revealed that treatment with the NF-κB inhibitor BAY11-7082 significantly inhibited the increase of PSGL-1 mRNA expression and, consequently the cell surface expression of PSGL-1, in U1 cells cocultured with FDCs (Fig. 4, *C* and *D*). This suggested a crucial role for NF-κB signaling in the induction of PSGL-1 during this coculture in HIV-1-infected cells. Likewise, we found that BAY11-7082 treatment also decreased the induction of P-selectin mRNA in FDCs, indicating that the NF-κB activation in FDCs could play

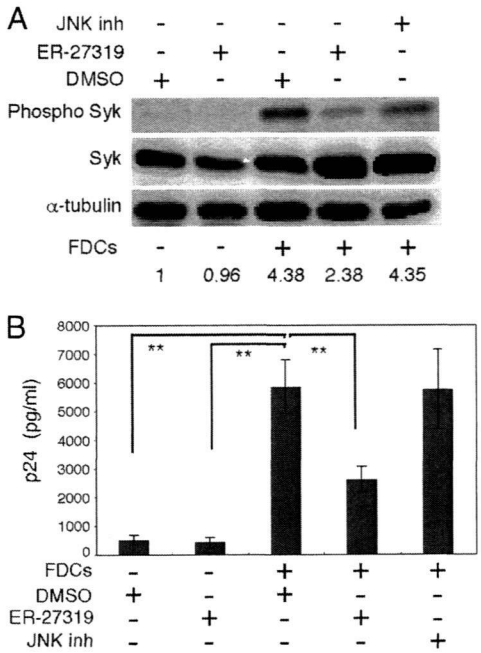

FIGURE 5. Syk is a mediator of P-selectin/PSGL-1 signaling for HIV-1 replication in U1 cells. *A* and *B*, U1 cells (1×10^5 cells/well) were untreated or pretreated with either ER-27319 (30 μM) or JNK inhibitor II (1 μM) for 1 h. Cells were then cocultured with FDCs (1×10^4 cells/well) for 3 days in the presence or absence of inhibitor. Cells were collected and subjected to immunoblotting analysis for phosphorylated Syk (Tyr^{352}), unmodified Syk, and α-tubulin (*A*). The numbers below the blot indicate the band intensity ratios. Cell supernatants were assayed for measurement of p24 (*B*). The data shown are the average ± SD of two independent experiments (*, $p \leq 0.05$ and **, $p \leq 0.01$ by the Student *t* test).

a crucial role in the induction of P-selectin during the coculture with HIV-1-infected monocytic cells (Fig. 4*E*).

Next, to test the biological significance of a P-selectin-PSGL-1 interaction in terms of HIV-1 induction in our FDC coculture system, U1 cells were pretreated with blocking Ab against PSGL-1 before setting up these cultures. Treatment with PSGL-1 Ab, but not an ICAM-1 Ab, specifically suppressed HIV-1 production in a dose-dependent manner (Fig. 4*F*). Consistent with this result, targeted disruption of PSGL-1 by specific siRNA significantly decreased HIV-1 production in U1 cells coculturing with FDCs (Fig. 4*G*). These results together indicate that a juxtacrine signaling mechanism mediated by PSGL-1/P-selectin underlies the activation of HIV-1 replication in infected monocytic cells stimulated by FDCs.

Syk acts as a downstream effector of PSGL-1 during HIV-1 replication

Several previous reports have demonstrated that the cytoplasmic domain of PSGL-1 can directly interact with a Src family kinase, the Syk (35). Syk consists of two N-terminal Src homology 2 domains, which bind phosphorylated ITAM sequences, and a C-terminal tyrosine kinase domain (35–37). The phosphorylation of Syk at Tyr^{352} has been shown to be a hallmark of its activation. Indeed, phosphorylated Syk was found in our present analyses to be significantly increased in U1 cells during their cocultivation with FDCs (Fig. 5*A*).

To next examine the possible biological functions of Syk during HIV-1 replication, we used a specific inhibitor of the molecule ER-27319 (29, 30) in our FDC cocultures. Treatment with ER-27319 significantly decreased HIV-1 production and this was accompanied by a reduction in the phosphorylated Syk levels in U1

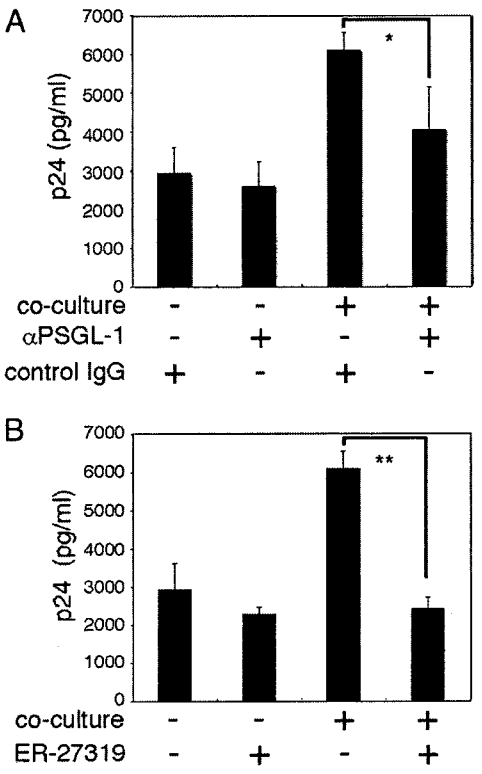

FIGURE 6. Inhibition of the PSGL-1/Syk pathway abrogates FDC-induced HIV-1 replication in primary monocytes. *A* and *B*, Primary human monocytes were separated from three healthy donors as indicated in *Materials and Methods* and these cells were then treated with 3 μg/ml PHA for 3 days. After stimulation, the cells (1×10^5 cells/well) were infected with HIV-$1_{JR\text{-}FL}$ (MOI = 0.05) for 24 h and subsequently cocultured with FDCs (1×10^4 cells/well) in the presence of PSGL-1 Ab (25 μg/ml; *A*) or ER-27319 (30 μM; *B*) at 14 days, followed by measurement of p24 (*, $p \leq 0.05$ and **, $p \leq 0.01$ by the Student t test).

cells (Fig. 5), whereas JNK inhibitor II had no such effects. These results indicate that the juxtacrine signaling between FDCs and HIV-1-infected monocytic cells mediated by P-selectin/PSGL-1 results in the activation of Syk, which serves as a mediator of the function of NF-κB activation in the HIV-1 replication pathway.

PSGL-1 and Syk inhibition blocks FDC-induced HIV-1 replication in primary monocytes

Finally, we addressed whether FDCs can also activate HIV-1 production in infected primary cells via P-selectin/PSGL-1 pathway, in this case human primary monocytes from healthy donors that had subsequently been exposed to HIV-$1_{JR\text{-}FL}$. At 24 h after viral infection, the primary monocytes were cocultured with FDCs in the presence or absence of either PSGL-1 Ab or the Syk inhibitor ER-27319. Both of these treatments significantly inhibited HIV-1 production in the primary monocytes in a manner similar to U1 cells (Fig. 6). These results indicate that similar to U1 cells, the PSGL-1/Syk signaling is likely to be a major pathway mediating FDC-induced HIV-1 replication in primary monocytes.

Discussion

Previous studies have indicated that HIV-1 infection is largely confined to the GCs of secondary lymph nodes where FDCs commonly reside (15–17). This microenvironment could thus provide the site for highly productive HIV-1 infection whereby FDCs might execute "on-switch" signaling to increase HIV replication. Furthermore, cell-cell infection appears to be far more efficient for viral spread than cell-free virus infection (38, 39). We here report that FDCs can facilitate HIV-1 replication in adjacent infected monocytes/macrophages via a cell-cell interaction mechanism.

FDCs have been shown to interact with B or $CD4^+$ T cells in the GCs of normal lymph nodes (16, 17, 20). It is also reported that in tonsils, CD150 $(SLAM)^+$ monocytes were localized not only in T cell areas, but also within GCs, suggesting they play a role in B cell activation (40). Moreover, substantial numbers of HIV-infected macrophages were observed in GCs during the course of HIV infection (41). Thus, FDCs can interact with HIV-infected monocytes or macrophages under these conditions during HIV-1 infection. Furthermore, the dysfunctional FDC network is observed in secondary lymph nodes of lymphadenopathy, where the degeneration of the FDC network is usually seen following highly active antiretroviral therapy or administration of therapeutic vaccine in HIV or SIV infection (42–45). One of the most common histological features of HIV-1-associated lymphadenopathy is hyperplastic lymphoid follicles that subsequently undergoes follicululolysis, in which FDCs can be scattered to the extra-GC within the lymph nodes such as cortical sinuses and mantle bodies (46, 47). Our results with immunohistochemical analysis indicate that FDCs reside with various types of HIV-1-infected cells including monocytes or macrophages in lymphoid organs of HIV-1-associated lymphadenopathy (supplemental Fig. 1). Therefore, our current proposed model for cell-cell interaction between FDCs and HIV-1-infected monocytic cells may reflect the biological or pathological aspects of the natural HIV infection in vivo. However, we could not determine the specific cell surface molecules for activating HIV-1 replication via the cell-cell interaction in vivo. Moreover, it is not well confirmed whether a multitude of other cells, cytokines, and other factors in vivo could influence the cell-cell interaction observed in our in vitro coculture system. Further careful analysis should be performed using human tissues as well as a humanized mouse model inoculated with HIV-1-infected human cells.

We clearly demonstrated here that FDCs, derived from human tonsils, can enhance HIV-1 production in infected monocytic cells in a coculture system. This enhancement requires direct cell-cell interactions via a juxtacrine signaling pathway that is mediated by P-selectin/PSGL-1. Our results are summarized as follows: 1) FDCs can activate HIV-1 replication in infected cells through cell-cell interactions; 2) HIV-1 replication is activated at the transcriptional level and is accompanied by the activation of the HIV-1 LTR through NF-κB; 3) P-selectin expression in FDCs and the up-regulation of its cognate receptor PSGL-1 in HIV-1-infected monocytes cells are facilitated via NF-κB activation; 4) the pathways leading to HIV-1 induction in cell lines also function in human primary monocytes and macrophages infected with HIV-1; and 5) selective inhibitors of PSGL-1 or Syk can efficiently block HIV-1 production in U1 and primary monocytes. These data together indicate for the first time that FDCs are a potent inducer of HIV-1 replication in surrounding infected monocytes and macrophages and that PSGL-1/Syk signaling plays a crucial role in this induction of HIV-1.

Very recently, Thacker et al. (26) reported a similar but distinct role of FDCs in the induction of HIV-1 replication in $CD4^+$ T cells obtained from PBMCs and GCs. We also confirmed that FDCs could stimulate HIV-1 replication in MOLT-4 T cells (23) as well as in primary $CD4^+$ T cells (data not shown). However, FDCs-induced HIV-1 replication in $CD4^+$ T cells might be mediated by a distinct mechanism from HIV-1-infected monocytic cells since the involvement of the PSGL-1/Syk pathway in $CD4^+$ T cells was found to be not prominent (K. Ohba, A. Ryo, and N. Yamamoto, unpublished observation). Therefore, the molecular mechanism for

FDCs to stimulate HIV-1 replication in surrounding infected cells could be attributable to cell type specific.

Intercellular interactions via a ligand/receptor juxtacrine signaling system has been implicated in several virus infections. Tsukamoto et al. (48) reported that the juxtacrine function of the IL-15/IL-15 receptor system in human B cell lines might play a role in the infectivity of EBV (48). Pilotti et al. (49) have demonstrated a crucial protective role for CCL3L1/CCL3 (MIP-1αP/LD78α) signals in both HIV infection and subsequent disease progression. These intercellular communication processes may play an important role in the sustained infection of viruses in different microenvironments within lymphoid organs. Further careful analyses will be required in the future to elucidate the variety of intercellular communication systems that may operate during HIV-1 infection.

There is now some evidence for a role of PSGL-1 as a signal-transmitting receptor in neutrophils (50), monocytes (51), and T lymphocytes (52). This molecule has been reported to associate with Syk through its interaction with moesin and promotes the tyrosine phosphorylation and thus the activation of Syk (35). In addition, signals elicited through PSGL-1/Syk can induce the activation of downstream effectors such as ERK, c-Fos, and NF-κB (53). The activation of NF-κB via PSGL-1 has also been demonstrated in platelet-stimulated monocytes, although the details of the molecular pathways leading to NF-κB activation in this manner have not yet been elucidated (51). Consistent with this result also, we found from our current analyses that PSGL-1/Syk signaling can activate NF-κB. This observation suggests a linkage between PSGL-1 signaling and HIV-1 replication through the activation of NF-κB.

Recently, Gilbert et al. (54) have reported that Src and Syk tyrosine kinases play important roles in the spread of HIV-1 from immature monocyte-derived DCs to $CD4^+$ T cells. They found that these kinases play a suppressive role in virus transfer in vitro probably by inhibiting the formation of the virological synapse. However, it has not been well characterized whether these signaling molecules contribute to the cell-cell interaction between HIV-1-infected cells and adjacent noninfected cells for virus replication. We showed in this current study that the activation of Syk through the PSGL-1 positively regulates HIV-1 replication in infected monocytic cells. Thus, Syk could be involved at multiple points in HIV-1 infection and its role could be dependent on each step of HIV-1 life cycle.

In summary, we demonstrate in our current study that FDCs are a potent activator of HIV-1 replication in surrounding infected monocytic cells. Furthermore, the PSGL-1/Syk pathway is important for this activation of HIV-1 replication. These results shed valuable new light on our understanding of the natural progression of HIV-1 infection over the long term and could provide a means for designing novel therapeutic interventions against AIDS and related disorders.

Acknowledgments

We thank S. Yamaoka and W. Sugiura for helpful discussions and H. Shimura, N. Sakamaki, C. Matsubara, M. Tanaka, and H. Soeda for technical assistance.

Disclosures

The authors have no financial conflict of interest.

References

1. Stevenson, M. 2003. HIV-1 pathogenesis. *Nat. Med.* 9: 853–860.
2. Pope, M., and A. T. Haase. 2003. Transmission, acute HIV-1 infection and the quest for strategies to prevent infection. *Nat. Med.* 9: 847–852.
3. Matsuyama, T., Y. Hamamoto, T. Okamoto, K. Shimotohno, N. Kobayashi, and N. Yamamoto. 1988. Tumour necrosis factor and HIV: a note of caution. *Lancet* 2: 1364.
4. Matsuyama, T., N. Kobayashi, and N. Yamamoto. 1991. Cytokines and HIV infection: is AIDS a tumor necrosis factor disease? *AIDS* 5: 1405–1417.
5. Kinter, A., J. Arthos, C. Cicala, and A. S. Fauci. 2000. Chemokines, cytokines and HIV: a complex network of interactions that influence HIV pathogenesis. *Immunol. Rev.* 177: 88–98.
6. Kedzierska, K., S. M. Crowe, S. Turville, and A. L. Cunningham. 2003. The influence of cytokines, chemokines and their receptors on HIV-1 replication in monocytes and macrophages. *Rev. Med. Virol.* 13: 39–56.
7. Pantaleo, G., C. Graziosi, J. F. Demarest, L. Butini, M. Montroni, C. H. Fox, J. M. Orenstein, D. P. Kotler, and A. S. Fauci. 1993. HIV infection is active and progressive in lymphoid tissue during the clinically latent stage of disease. *Nature* 362: 355–358.
8. Pierson, T., J. McArthur, and R. F. Siliciano. 2000. Reservoirs for HIV-1: mechanisms for viral persistence in the presence of antiviral immune responses and antiretroviral therapy. *Annu. Rev. Immunol.* 18: 665–708.
9. Han, Y., M. Wind-Rotolo, H. C. Yang, J. D. Siliciano, and R. F. Siliciano. 2007. Experimental approaches to the study of HIV-1 latency. *Nat. Rev. Microbiol.* 5: 95–106.
10. Pauza, C. D. 1988. HIV persistence in monocytes leads to pathogenesis and AIDS. *Cell. Immunol.* 112: 414–424.
11. Igarashi, T., C. R. Brown, Y. Endo, A. Buckler-White, R. Plishka, N. Bischofberger, V. Hirsch, and M. A. Martin. 2001. Macrophage are the principal reservoir and sustain high virus loads in rhesus macaques after the depletion of $CD4^+$ T cells by a highly pathogenic simian immunodeficiency virus/HIV type 1 chimera (SHIV): Implications for HIV-1 infections of humans. *Proc. Natl. Acad. Sci. USA* 98: 658–663.
12. Moser, B., and P. Loetscher. 2001. Lymphocyte traffic control by chemokines. *Nat. Immunol.* 2: 123–128.
13. Cahalan, M. D., and G. A. Gutman. 2006. The sense of place in the immune system. *Nat. Immunol.* 7: 329–332.
14. Bieniasz, P. D. 2004. Intrinsic immunity: a front-line defense against viral attack. *Nat. Immunol.* 5: 1109–1115.
15. Allen, C. D., T. Okada, and J. G. Cyster. 2007. Germinal-center organization and cellular dynamics. *Immunity* 27: 190–202.
16. Szakal, A. K., Y. Aydar, P. Balogh, and J. G. Tew. 2002. Molecular interactions of FDCs with B cells in aging. *Semin. Immunol.* 14: 267–274.
17. van Nierop, K., and C. de Groot. 2002. Human follicular dendritic cells: function, origin and development. *Semin. Immunol.* 14: 251–257.
18. Victoratos, P., J. Lagnel, S. Tzima, M. B. Alimzhanov, K. Rajewsky, M. Pasparakis, and G. Kollias. 2006. FDC-specific functions of p55TNFR and IKK2 in the development of FDC networks and of antibody responses. *Immunity* 24: 65–77.
19. Tew, J. G., J. Wu, M. Fakher, A. K. Szakal, and D. Qin. 2001. Follicular dendritic cells: beyond the necessity of T-cell help. *Trends Immunol.* 22: 361–367.
20. Li, L., and Y. S. Choi. 2002. Follicular dendritic cell-signaling molecules required for proliferation and differentiation of GC-B cells. *Semin. Immunol.* 14: 259–266.
21. Lee, I. Y., E. M. Ko, S. H. Kim, D. I. Jeoung, and J. Choe. 2005. Human follicular dendritic cells express prostacyclin synthase: a novel mechanism to control T cell numbers in the germinal center. *J. Immunol.* 175: 1658–1664.
22. Keele, B. F., L. Tazi, S. Gartner, Y. Liu, T. B. Burgon, J. D. Estes, T. C. Thacker, K. A. Crandall, J. C. McArthur, and G. F. Burton. 2008. Characterization of the follicular dendritic cell reservoir of human immunodeficiency virus type 1. *J. Virol.* 82: 5548–5561.
23. Taruishi, M., K. Terashima, Z. Dewan, N. Yamamoto, S. Ikeda, D. Kobayashi, Y. Eishi, M. Yamazaki, T. Furusaka, M. Sugimoto, et al. 2004. Role of follicular dendritic cells in the early HIV-1 infection: in vitro model without specific antibody. *Microbiol. Immunol.* 48: 693–702.
24. Burton, G. F., B. F. Keele, J. D. Estes, T. C. Thacker, and S. Gartner. 2002. Follicular dendritic cell contributions to HIV pathogenesis. *Semin. Immunol.* 14: 275–284.
25. Grouard, G., and E. A. Clark. 1997. Role of dendritic and follicular dendritic cells in HIV infection and pathogenesis. *Curr. Opin. Immunol.* 9: 563–567.
26. Thacker, T. C., X. Zhou, J. D. Estes, Y. Jiang, B. F. Keele, T. S. Elton, and G. F. Burton. 2009. Follicular dendritic cells and human immunodeficiency virus type 1 transcription in $CD4^+$ T cells. *J. Virol.* 83: 150–158.
27. Folks, T. M., J. Justement, A. Kinter, C. A. Dinarello, and A. S. Fauci. 1987. Cytokine-induced expression of HIV-1 in a chronically infected promonocyte cell line. *Science* 238: 800–802.
28. Watanabe, S., K. Terashima, S. Ohta, S. Horibata, M. Yajima, Y. Shiozawa, M. Z. Dewan, Z. Yu, M. Ito, T. Morio, et al. 2007. Hematopoietic stem cell-engrafted NOD/SCID/IL2Rγ null mice develop human lymphoid systems and induce long-lasting HIV-1 infection with specific humoral immune responses. *Blood* 109: 212–218.
29. Moriya, K., J. Rivera, S. Odom, Y. Sakuma, K. Muramato, T. Yoshiuchi, M. Miyamoto, and K. Yamada. 1997. ER-27319, an acridone-related compound, inhibits release of antigen-induced allergic mediators from mast cells by selective inhibition of Fcε receptor I-mediated activation of Syk. *Proc. Natl. Acad. Sci. USA* 94: 12539–12544.
30. Andrews, R. P., C. L. Kepley, L. Youssef, B. S. Wilson, and J. M. Oliver. 2001. Regulation of the very late antigen-4-mediated adhesive activity of normal and nonreleaser basophils: roles for Src, Syk, and phosphatidylinositol 3-kinase. *J. Leukocyte Biol.* 70: 776–782.
31. Cullen, B. R. 1991. Regulation of HIV-1 gene expression. *FASEB J.* 5: 2361–2368.

32. Rohr, O., C. Marban, D. Aunis, and E. Schaeffer. 2003. Regulation of HIV-1 gene transcription: from lymphocytes to microglial cells. *J. Leukocyte Biol.* 74: 736–749.
33. Okamoto, T., T. Matsuyama, S. Mori, Y. Hamamoto, N. Kobayashi, N. Yamamoto, S. F. Josephs, F. Wong-Staal, and K. Shimotohno. 1989. Augmentation of human immunodeficiency virus type 1 gene expression by tumor necrosis factor α. *AIDS Res. Hum Retroviruses* 5: 131–138.
34. Takada, N., T. Sanda, H. Okamoto, J. P. Yang, K. Asamitsu, L. Sarol, G. Kimura, H. Uranishi, T. Tetsuka, and T. Okamoto. 2002. RelA-associated inhibitor blocks transcription of human immunodeficiency virus type 1 by inhibiting NF-κB and Sp1 actions. *J. Virol.* 76: 8019–8030.
35. Urzainqui, A., J. M. Serrador, F. Viedma, M. Yanez-Mo, A. Rodriguez, A. L. Corbi, J. L. Alonso-Lebrero, A. Luque, M. Deckert, J. Vazquez, and F. Sanchez-Madrid. 2002. ITAM-based interaction of ERM proteins with Syk mediates signaling by the leukocyte adhesion receptor PSGL-1. *Immunity* 17: 401–412.
36. Fodor, S., Z. Jakus, and A. Mocsai. 2006. ITAM-based signaling beyond the adaptive immune response. *Immunol. Lett.* 104: 29–37.
37. Underhill, D. M., and H. S. Goodridge. 2007. The many faces of ITAMs. *Trends Immunol.* 28: 66–73.
38. Dimitrov, D. S., R. L. Willey, H. Sato, L. J. Chang, R. Blumenthal, and M. A. Martin. 1993. Quantitation of human immunodeficiency virus type 1 infection kinetics. *J. Virol.* 67: 2182–2190.
39. Chancey, C. J., K. V. Khanna, J. F. Seegers, G. W. Zhang, J. Hildreth, A. Langan, and R. B. Markham. 2006. Lactobacilli-expressed single-chain variable fragment (scFv) specific for intercellular adhesion molecule 1 (ICAM-1) blocks cell-associated HIV-1 transmission across a cervical epithelial monolayer. *J. Immunol.* 176: 5627–5636.
40. Farina, C., D. Theil, B. Semlinger, R. Hohlfeld, and E. Meinl. 2004. Distinct responses of monocytes to Toll-like receptor ligands and inflammatory cytokines. *Int. Immunol.* 16: 799–809.
41. Eitner, F., Y. Cui, G. Grouard-Vogel, K. L. Hudkins, A. Schmidt, T. Birkebak, M. B. Agy, S. L. Hu, W. R. Morton, D. M. Anderson, et al. 2000. Rapid shift from virally infected cells to germinal center-retained virus after HIV-2 infection of macaques. *Am. J. Pathol.* 156: 1197–1207.
42. Gray, C. M., J. Lawrence, E. A. Ranheim, M. Vierra, M. Zupancic, M. Winters, J. Altman, J. Montoya, A. Zolopa, J. Schapiro, et al. 2000. Highly active antiretroviral therapy results in HIV type 1 suppression in lymph nodes, increased pools of naive T cells, decreased pools of activated T cells, and diminished frequencies of peripheral activated HIV type 1-specific $CD8^+$ T cells. *AIDS Res. Hum Retroviruses* 16: 1357–1369.
43. Lu, W., X. Wu, Y. Lu, W. Guo, and J. M. Andrieu. 2003. Therapeutic dendritic-cell vaccine for simian AIDS. *Nat. Med.* 9: 27–32.
44. Schmitz, J., J. van Lunzen, K. Tenner-Racz, G. Grossschupff, P. Racz, H. Schmitz, M. Dietrich, and F. T. Hufert. 1994. Follicular dendritic cells retain HIV-1 particles on their plasma membrane, but are not productively infected in asymptomatic patients with follicular hyperplasia. *J. Immunol.* 153: 1352–1359.
45. Zhang, Z. Q., T. Schuler, W. Cavert, D. W. Notermans, K. Gebhard, K. Henry, D. V. Havlir, H. F. Gunthard, J. K. Wong, S. Little, et al. 1999. Reversibility of the pathological changes in the follicular dendritic cell network with treatment of HIV-1 infection. *Proc. Natl. Acad. Sci. USA* 96: 5169–5172.
46. Baroni, C. D., and S. Uccini. 1990. Lymph nodes in HIV-positive drug abusers with persistent generalized lymphadenopathy: histology, immunohistochemistry, and pathogenetic correlations. *Prog. AIDS Pathol.* 2: 33–50.
47. Houn, H. Y., A. A. Pappas, and E. M. Walker, Jr. 1990. Lymph node pathology of acquired immunodeficiency syndrome (AIDS). *Ann. Clin. Lab. Sci.* 20: 337–342.
48. Tsukamoto, K., Y. C. Huang, W. C. Dorsey, B. Carns, and V. Sharma. 2006. Juxtacrine function of interleukin-15/interleukin-15 receptor system in tumour derived human B-cell lines. *Clin. Exp. Immunol.* 146: 559–566.
49. Pilotti, E., L. Elviri, E. Vicenzi, U. Bertazzoni, M. C. Re, S. Allibardi, G. Poli, and C. Casoli. 2007. Postgenomic up-regulation of CCL3L1 expression in HTLV-2-infected persons curtails HIV-1 replication. *Blood* 109: 1850–1856.
50. Hidari, K. I., A. S. Weyrich, G. A. Zimmerman, and R. P. McEver. 1997. Engagement of P-selectin glycoprotein ligand-1 enhances tyrosine phosphorylation and activates mitogen-activated protein kinases in human neutrophils. *J. Biol. Chem.* 272: 28750–28756.
51. Weyrich, A. S., T. M. McIntyre, R. P. McEver, S. M. Prescott, and G. A. Zimmerman. 1995. Monocyte tethering by P-selectin regulates monocyte chemotactic protein-1 and tumor necrosis factor-α secretion: signal integration and NF-κB translocation. *J. Clin. Invest.* 95: 2297–2303.
52. Damle, N. K., K. Klussman, M. T. Dietsch, N. Mohagheghpour, and A. Aruffo. 1992. GMP-140 (P-selectin/CD62) binds to chronically stimulated but not resting $CD4^+$ T lymphocytes and regulates their production of proinflammatory cytokines. *Eur. J. Immunol.* 22: 1789–1793.
53. Tada, J., M. Omine, T. Suda, and N. Yamaguchi. 1999. A common signaling pathway via Syk and Lyn tyrosine kinases generated from capping of the sialomucins CD34 and CD43 in immature hematopoietic cells. *Blood* 93: 3723–3735.
54. Gilbert, C., C. Barat, R. Cantin, and M. J. Tremblay. 2007. Involvement of Src and Syk tyrosine kinases in HIV-1 transfer from dendritic cells to $CD4^+$ T lymphocytes. *J. Immunol.* 178: 2862–2871.

Vaccine 27 (2009) 5982–5988

Contents lists available at ScienceDirect

Vaccine

journal homepage: www.elsevier.com/locate/vaccine

Oral MucoRice expressing double-mutant cholera toxin A and B subunits induces toxin-specific neutralising immunity

Yoshikazu Yuki[a,*,1], Daisuke Tokuhara[a,1], Tomonori Nochi[a], Hiroshi Yasuda[b], Mio Mejima[a], Shiho Kurokawa[a], Yuko Takahashi[a], Nobuhiro Kataoka[a], Ushio Nakanishi[a], Yukari Hagiwara[c], Kohtaro Fujihashi[d], Fumio Takaiwa[e], Hiroshi Kiyono[a,d,*]

[a] The Institute of Medical Science, The University of Tokyo, Tokyo 108-8639, Japan
[b] National Agricultural Research Center for Hokkaido Region, Sapporo 062-8555, Japan
[c] Kitasato Institute Research Center for Biologicals, Saitama 364-0026, Japan
[d] Immunobiology Vaccine Center, Department of Pediatric Dentistry, The University of Alabama at Birmingham, Birmingham, AL 35294-0007, USA
[e] National Institute of Agrobiological Sciences, Tsukuba 305-8602, Japan

ARTICLE INFO

Article history:
Received 30 April 2009
Received in revised form 10 July 2009
Accepted 22 July 2009
Available online 7 August 2009

Keywords:
Rice-based vaccine
MucoRice
Oral vaccine
Cholera
Cold-chain-free
Mutant cholera toxin

ABSTRACT

Rice-expressed cholera toxin B (CTB) subunit is a cold-chain-free oral vaccine that effectively induces enterotoxin-neutralising immunity. We created another rice-based vaccine, MucoRice, expressing non-toxic double-mutant cholera toxin (dmCT) with CTA and CTB subunits. Western-blot analysis suggested that MucoRice-dmCT had the shape of a multicomponent vaccine. Oral administration of MucoRice-dmCT induced CTB- but not CTA-specific serum IgG and mucosal IgA antibodies, generating protective immunity against cholera toxin without inducing rice-protein-specific antibody responses. The potency of MucoRice-dmCT was equal to that of MucoRice-CTB vaccine. MucoRice has the potential to be used as a safe multicomponent vaccine expression system.

1. Introduction

To prepare for the successful execution of future global vaccination programs, it is essential that we consider creating a new generation of vaccines that do not require refrigeration storage and traditional syringes and needles for vaccination. The use of transgenic plant-derived recombinant protein is a promising strategy that combines innovation and knowledge of mucosal immunology and plant biotechnology to produce such suitable plant-based vaccines for global immunisation [1,2]. The potential benefits include cost-effective and rapid up-scaling of production, expression of multiple genes at one time, and lower risk of contamination with human pathogens in the preparation of vaccine antigens. Furthermore, plants are suitable for foreign protein production and storage and as oral delivery options for subunit-type vaccines to induce protective immunity against infectious diseases via the mucosal immune system [1,2]. Among several plant-based vaccines developed, grains such as corn, wheat and rice have recently attracted interest for vaccine production, storage and delivery systems for oral immunisation. As a vaccine antigen production system, rice seed has advantages over other grains, including easier storage and processing and greater yield; moreover, the rice plant has self-crossing ability [3]. In addition, a rice transformation system has been established and the full genome sequence elucidated, enabling rice genetic information to be easily applied to the creation of a gene-manipulated product [3,4].

We recently developed a rice-based oral cholera toxin (CT) B (CTB)-subunit vaccine (MucoRice-CTB) that has many practical advantages over most traditional injection-type vaccines and other plant-based oral vaccines [3]. The rice-based oral vaccine is stable at room temperature for several years and is protected from digestive enzymes in the harsh conditions of the gastrointestinal tract. When MucoRice-CTB was given orally, the vaccine induced antigen-specific antibodies with toxin-neutralising activity [3]. Here, to demonstrate the development of a multicomponent vaccine as part of a rice-based vaccine antigen expression system, we produced transgenic rice seed expressing the A and B subunits

* Corresponding authors. Tel.: +81 1 5449 5274; fax: +81 1 5449 5411.
E-mail addresses: yukiy@ims.u-tokyo.ac.jp (Y. Yuki), kiyono@ims.u-tokyo.ac.jp (H. Kiyono).
[1] These authors contributed equally to this work and share first authorship.

0264-410X/$ – see front matter © 2009 Elsevier Ltd. All rights reserved.
doi:10.1016/j.vaccine.2009.07.071

of a nontoxic double-mutant cholera toxin (dmCT), which contained two amino acid substitutions, of the ADP-ribosyltransferase active centre (E112K) and carboxyl-terminal KDEL (E112K/KDGL) in the A subunit (dmCTA) [5,6]. We then examined whether oral vaccination with this seed would effectively induce enterotoxin-neutralising immunity. Although dmCT is considered safe and nontoxic, exhibiting no ADP-ribosyltransferase activity and participating in normal intracellular trafficking [6], it retains the biological capacity to enhance antibody immune responses against co-administered antigens [6]. Our strategy was aimed at utilising these unique characteristics of dmCT by inserting a dmCTA-specific gene into the rice genome to develop rice expressing dmCTA in addition to the original CTB, thus yielding a multicomponent vaccine, MucoRice-dmCT.

2. Materials and methods

2.1. DNA construction and transformation of rice plants

A double mutant of the CT gene (dmCT E112K/KDGL) was modified to a suitable codon optimisation form for rice seed by introducing two potent mutations into the ADP-ribosylation activity centre and C-terminal KDEL [6,7]. The modified dmCTA subunit and B-subunit genes for the dmCT gene were cloned as individual ORFs flanked with plant elements to facilitate the transcription of each subunit. The dmCTA subunit and dmCT cassettes were assembled. The dmCTA subunit cassette consisted of a *GluB-4* promoter/signal sequence followed by the rice-optimised dmCTA (E112K/KDGL) with a Nos terminator [8]. The dmCT cassette consisted of both a dmCTA subunit cassette and a B subunit cassette, which comprised a GluB-1 promoter/signal sequence followed by a rice-optimised B subunit with a GluB-1 terminator [8]. Finally, each cassette was cloned into the binary vector pGPTV-35S-HPT [4]. The resulting plasmids for dmCT and dmCTA were individually transformed in rice plants, *Oryza sativa* L. 'Kita-ake' [9], by using an *Agrobacterium*-mediated method described previously [10]. Rice-expressed CTB with a KDEL signal at the C-terminal of CTB was produced as reported previously [3].

2.2. DNA and protein analyses

Using the cetyltrimethylammonium bromide (CTAB) extraction method, genomic DNA was extracted from the leaf tissues of transgenic rice, and the integration of the dmCT gene into the genomic DNA was analysed by PCR [4]. Total seed protein was extracted from the seeds as described previously [3]. Briefly, seeds of rice plants were ground to a fine powder by using a Multi-Beads Shocker (Yasui Kikai, Osaka, Japan). Seeds were extracted under reducing conditions in 2% (w/v) SDS, 8 M urea, 5% (w/v) β-mercaptoethanol, 50 mM Tris–HCl (pH 6.8) and 20% (w/v) glycerol before being separated by SDS-PAGE with a 15–25% gradient polyacrylamide gel (Daiichi Pure Chemical, Tokyo, Japan). Under non-reducing conditions, seeds were extracted in 0.1% (w/v) SDS, 50 mM Tris–HCl (pH 6.8) and 20% (w/v) glycerol before being separated by SDS-PAGE. The gel was subsequently transferred to Hybond-P PVDF membranes (GE Healthcare) for Western-blot analysis with 5 μg/ml rabbit anti-mCTA antibody or rabbit anti-CTB prepared in our laboratory. Accumulation levels of CTA or CTB were determined by densitometric analysis of the Western blots against a standard curve generated with the use of rmCTA (E112K) or rCTB expressed in *Bacillus brevis* and purified in our laboratory [5,11,12]. Antibody to rmCTA or rCTB was raised from rabbits immunised with the respective recombinant protein in our laboratory.

2.3. Oral immunisation and assessment of antibody responses by ELISA

An oral immunisation study was performed in 6-week-old BALB/c mice (CLEA, Tokyo, Japan). On five occasions at 2-week intervals, mice (five mice per group) were orally immunised with 50 mg of CTB-transgenic rice, with a corresponding dose of CTB at 75 μg; or with 200 mg of dmCT-transgenic rice, with a corresponding dose of dmCTA at 20 μg and CTB at 50 μg; or with 50 mg of CTB-transgenic rice plus 200 mg of dmCTA-transgenic rice, with a corresponding dose of CTB at 75 μg plus dmCTA at 10 μg; or with 250 mg of dmCTA-transgenic rice, with a corresponding dose of dmCTA at 12.5 μg; or with either 200 mg of non-transgenic rice dissolved in 1 ml of PBS or with PBS alone, as controls. To examine the adjuvant effect of transgenic rice, mice were orally immunised three occasions at a week interval with 250 μg tetanus toxoid (TT, kindly provided by The Research Foundation for Microbial Diseases of Osaka University, Suita, Osaka, Japan) alone in 1 ml of PBS or with TT together with 200 mg of rice-expressed dmCT, 100 mg of rice-expressed CTB, 200 mg of wild-type (WT) rice or 10 μg of CT (List Biological Laboratories, Campbell, CA). One week after the final immunisation, serum and faecal extracts were collected and CTB-, CTA-, TT- or rice-storage protein-specific immunoglobulin responses were measured by ELISA with 5 μg/ml of rCTB, rmCTA or TT or 20 μg/ml rice-storage protein extracted with 0.01% Triton X-100, as described previously [3].

2.4. Analyses of neutralising antibody and protection activity

CT (50 ng/ml) was added to serially diluted sera collected from immunised mice. The sera were then subjected to GM1-ELISA as previously described, with some modifications [13]. Briefly, 96-well plates (Thermo, Milford, MA) coated with 5 μg/ml of monosialoganglioside GM1 (Sigma) were incubated with CT that had first been treated with serum from immunised mice and then with an HRP-conjugated Rabbit anti-CTB antibody prepared in our laboratory [3]. The colour of the solutions was developed by the addition of TMB substrate (Moss, Pasadena, MD), and absorbance was measured at a wavelength of 450 nm. In addition, a CHO cell (line ATCC, CCL-61) assay [14] was performed with serum to which 50 ng/ml of CT had been added. After 14 h of stimulation of the cells in 5% CO_2 in a humidified incubator at 37 °C, morphological changes were observed under a microscope. In addition, we performed an *in vivo* challenge experiment with CT, as described previously [3]. The vaccinated mice were orally challenged with 20 μg of CT. After 14 h the mice were examined for clinical signs of diarrhoea and the volume of intestinal water was measured.

2.5. Data analysis

Data were expressed as means ± standard deviation. All analyses for statistically significant differences were performed with Tukey's *t* test, with P values < 0.01 considered to indicate significance (**).

3. Results

3.1. Development of rice-expressed nontoxic double-mutant cholera toxin (dmCT)

The two genes encoding dmCTA and CTB were generated as shown in Fig. 1. We chose to introduce the dmCTA and CTB genes separately into the same rice as rice-expressed dmCT in order to prove the antigenicity, and lack of adjuvanticity, of dmCT. Using codons preferentially used for translation of several rice-seed-protein genes, both genes were optimised for expression in the

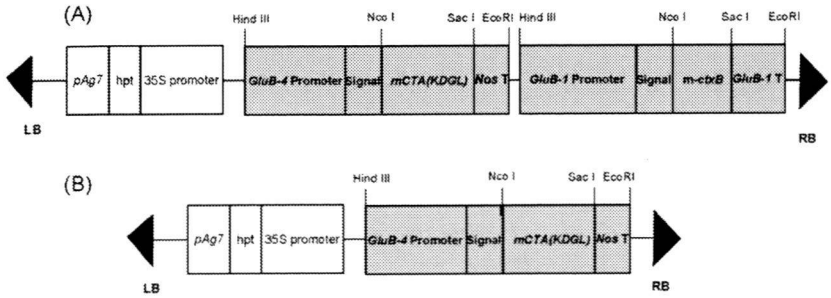

Fig. 1. Schematic representation of transformation plasmids for the development of MucoRice-dmCT. The DNA fragments coding dmCT (A) and dmCTA (B) were placed under the control of the rice-seed major storage protein glutelin GluB-4 promoter and/or glutelin GluB-1 promoter. 35S promoter: Cauliflower mosaic virus 35S promoter; hpt: hygromycin phosphotransferase gene; LB: left border; pAg7: agropine synthase polyadenylation signal sequence; RB: right border.

transgenic rice seed. Rice seed storage protein glutelin 1.4-kb GluB-4 promoter/signal peptides and 2.3-kb GluB-1 promoter/signal peptides were translationally fused to the dmCTA and CTB genes, respectively, to achieve endosperm-specific expression. The dmCT (dmCTA and CTB) or dmCTA alone of these chimeric genes was cloned into the plant expression vector pGPTV-35S-HPT (Fig. 1A, dmCT; Fig. 1B, dmCTA). Following *Agrobacterium*-mediated transformation of Kita-ake rice plants, several independent transgenic rice lines were generated for each of the two constructs (dmCT and dmCTA), and accumulation levels in the seed were examined by immunoblot analysis. For each antigen, one plant line that had the highest levels of antigen accumulated in the seed was selected and proceeded to the T3 generation by self-crossing to obtain homozygous lines. Integration of the dmCTA and CTB genes into the rice genome was examined by PCR amplification; each gene was PCR-amplified in the plant line in the case of the dmCTA or CTB construct, whereas no signal was amplified in non-transgenic rice (data not shown).

To examine the accumulation of dmCTA and CTB in transgenic rice seed, total seed protein was extracted under either reducing (Fig. 2A and B) or non-reducing (Fig. 2C and D) conditions from mature seed and analysed by SDS-PAGE followed by Western blotting analysis with anti-rmCTA (Fig. 2 B and D) or anti-rCTB (Fig. 2A and C) antibodies. Under reducing conditions, a 26-kDa band was recognised by the mCTA-specific antibody in the total seed protein of the dmCT and dmCTA lines (Fig. 2B), whereas authentic cholera toxin gave two bands, at 26 and 20 kDa, which corresponded to CTA and CTA1, respectively (Fig. 2B). CTA is synthesised with a trypsin-sensitive bond that joins the CTA1 and CTA2 pieces; each piece is itself bonded to the other with a disulphide bond [15]. In the dmCT and CTB lines, 11-kDa and 14-kDa bands were detected by CTB-specific antibody; however, the accumulation levels of CTB in the dmCT line were less than those in the CTB line (Fig. 2A). The 14-kDa bands estimated from electrophoresis were larger than the authentic and monomeric CTB band (10 kDa), probably because of the addition of all, or part of, the *GluB-1* signal peptide at the N-terminus of CTB and/or plant-based glycosylation.

Under non-reducing conditions, several bands of CTB protein of high molecular weight (about 37–50 kDa) were detected in the total seed protein from dmCT and CTB lines by Western-blot analysis with CTB-specific antibody (Fig. 2C). These findings indicated that CTB proteins were produced and accumulated in both transgenic rice lines of MucoRice-dmCT and -CTB as part of the assembly of the pentameric structure, which consisted of two types of monomer. Unlike the case with authentic CT, a 60-kDa band was not detected with either anti-CTA (Fig. 2C) or anti-CTB (Fig. 2D) antibodies when MucoRice-dmCT was examined, suggesting that the mutant toxin assembled in MucoRice-dmCT was not of authentic size. However, notably, the two subunits were definitively and independently expressed in the transgenic rice seed.

The levels of accumulation of dmCT and dmCTA expressed in the seeds were quantified by densitometric analysis with known amounts of purified rmCTA and rCTB as standards (data not shown). CTB was accumulated in rice-expressed dmCT at 5 μg per seed, whereas the quantity of rice-expressed CTB with the KDEL signal was as high as 30 μg per seed. CTA accumulated in rice-expressed dmCT at 2 μg per seed and in rice-expressed dmCTA at 1 μg per seed. The differences in expression level between dmCT and

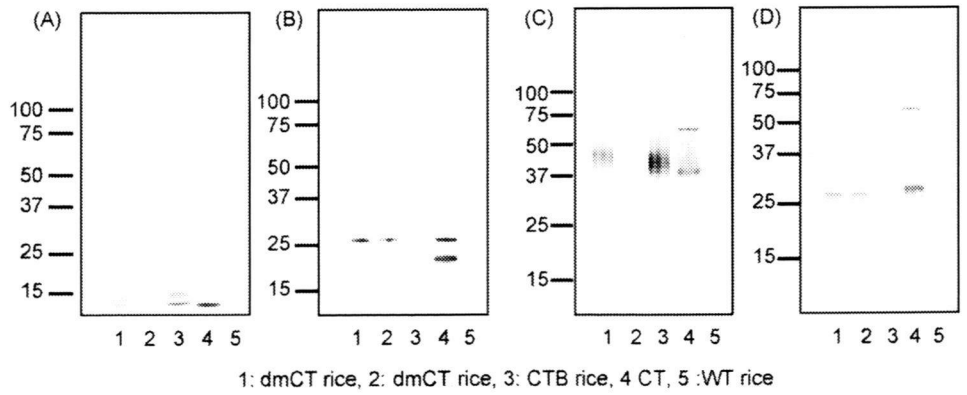

Fig. 2. Analysis of CT subunit expression in MucoRice-dmCT. Western-blot analysis under reducing conditions (A and B) revealed that rice-expressed dmCT and CTB gave 11-kDa and 14-kDa bands on detection with specific anti-CT-B antibody (A), and rice-expressed dmCT and CTA gave 26-kDa bands on detection with specific anti-CTA antibody (B), whereas authentic CT gave an 11-kDa band for CTB, and 26-kDa and 20-kDa bands for CTA and CTA1, respectively (A and B). Western-blot analysis under non-reducing conditions (C and D) revealed that rice-expressed dmCT and -CTB gave 37–50-kDa bands upon detection with specific anti-CT-B antibody (C), and rice-expressed dmCT and CTA gave a 26-kDa band on the detection with specific anti-CTA antibody (D), whereas authentic CT gave bands of 26–kDa (CTA), 37–50-kDa (CTB pentamer), and 60–kDa (CT) (C and D).

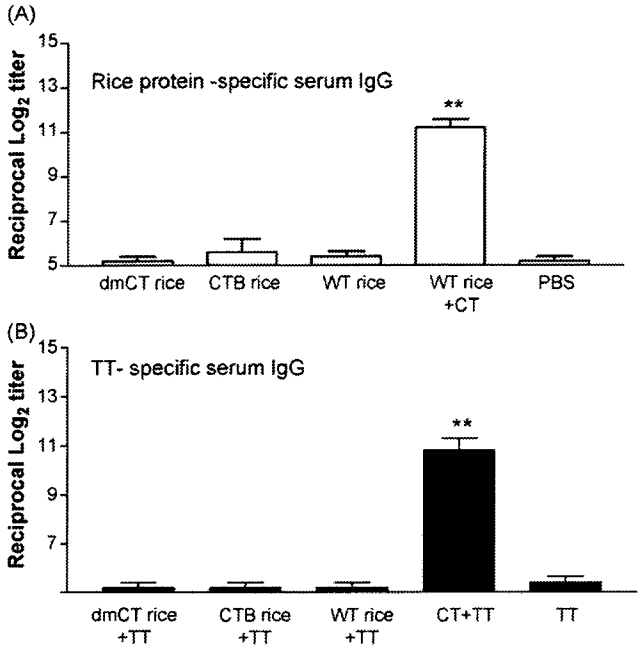

Fig. 3. Lack of adjuvant activity by MucoRice-dmCT. Mice were immunised with rice-expressed dmCT (200 mg power containing 20 μg of dmCTA and 50 μg of CTB), CTB (100 mg power containing 150 μg of CTB), wild-type (WT) rice (200 mg powder), WT rice (200 mg powder) together with 10 μg of CT dissolved in PBS, or PBS alone as a control. Rice-storage-protein-specific IgG responses were not induced in mice immunised with rice-expressed dmCT, CTB, or WT rice or PBS, but they were induced in mice that received WT rice together with CT (A). Mice were immunised with TT (250 μg) alone dissolved in PBS as a control, or the same amount of TT together with rice-expressed dmCT (200 mg power), CTB (100 mg power), WT rice (200 mg powder), or CT (10 μg). TT-specific IgG responses were not induced in mice immunised with TT alone or with TT together with rice-expressed dmCT, CTB, or WT rice. They were induced in mice that received TT together with CT (B).

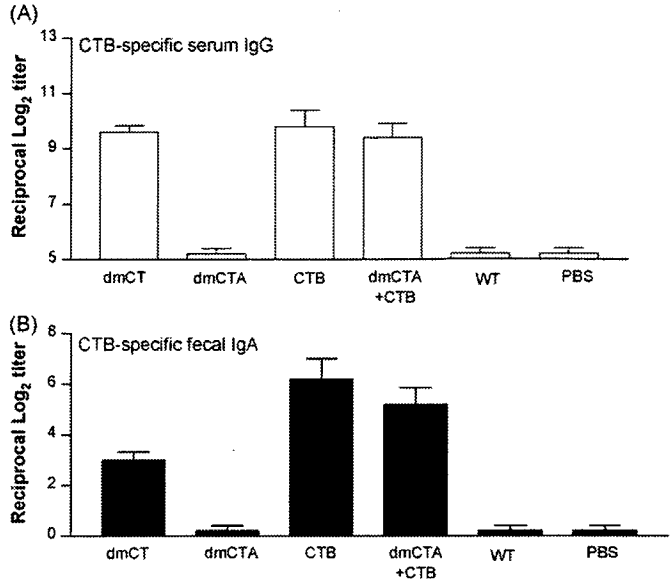

Fig. 4. Induction of CTB-specific antibody responses in mice orally immunised with MucoRice-dmCT. Mice were immunised with rice-expressed dmCT (200 mg power containing 20 μg of dmCTA and 50 μg of CTB), dmCTA (250 mg power containing 12.5 μg of mCTA), CTB (50 mg power containing 75 μg of CT-B), dmCTA (200 mg power containing 10 μg of dmCTA) plus CTB (50 mg power containing 75 μg of CTB), wild-type (WT) rice (200 mg powder) dissolved in PBS, or PBS alone as a control. Equal CTB-specific IgG responses were induced in mice immunised with rice-expressed dmCT, CTB, or dmCT plus CTB, but not in mice that received dmCTA, WT rice, or PBS alone (A). CTB-specific faecal IgA responses were also induced in mice immunised with rice-expressed dmCT, CTB, or dmCT plus CTB, but this mucosal response depended on the dose of CTB (B).

CTB rice may be related to the presence or absence of the KDEL signal.

3.2. *Rice-expressed dmCT induces no rice-protein- or co-administered TT-specific immune responses after oral administration*

Because dmCT is known to be an effective mucosal adjuvant when administered nasally, we first examined whether rice-expressed dmCT would induce rice-protein-specific immune responses. Oral administration of MucoRice-dmCT or -CTB did not induce rice-storage protein-specific antibody immune responses (Fig. 3A). This finding suggested that, like MucoRice-CTB, MucoRice-dmCT had no mucosal adjuvant activity. This finding was further confirmed by the results of an oral immunisation study with 250 μg of TT plus either MucoRice-dmCT, MucoRice-CTB or WT rice. None of the co-administered rice preparations supported the generation of TT-specific antibody immune responses (Fig. 3B). In contrast, oral immunisation of a group of mice with TT and CT induced antigen-specific IgG antibody responses to the co-administered protein vaccine antigen (Fig. 3A and B). These findings demonstrated that rice-expressed dmCT (or CTB) showed no adjuvanticity to co-administered TT or to rice protein.

3.3. *Rice-expressed dmCT induces CTB- but not CTA-specific immune responses in both systemic and mucosal compartments after oral administration*

To examine the oral immunogenicity of MucoRice-dmCT, mice were orally immunised with seed powders prepared from MucoRice expressing dmCT, dmCTA, CTB or dmCTA plus CTB, or from WT rice. CTB-specific serum IgG and mucosal IgA antibodies were detected in mice immunised with 200 mg (20 μg of dmCTA and 50 μg of CTB) of MucoRice-dmCT, 50 mg (75 μg of CTB) of MucoRice-CTB or 200 mg (10 μg of dmCTA) of MucoRice-dmCTA plus 50 mg (75 μg of CTB) of MucoRice-CTB (Fig. 4). The difference between the rice-expressed dmCT and CTB in terms of induction of CTB-specific mucosal IgA antibody response depended on the level of expression of CTB. CTA-specific serum IgG or mucosal IgA antibodies were not detected in mice immunised with seed powders prepared from all transgenic rice lines including 250 mg (12.5 μg of dmCTA) of MucoRice-dmCTA or 200 mg (20 μg of dmCTA) of MucoRice-dmCT (data not shown).

3.4. *Rice-expressed dmCT induces protective immunity against CT*

To examine the biological activity of CTB-specific antibodies induced by oral administration of MucoRice-dmCT or MucoRice-CTB, CT-neutralising activities were investigated by using a GM1-binding inhibition assay with GM1-ELISA and an elongation assay with CHO cells. As negative controls we used serum antibodies from mice orally immunised with MucoRice-dmCTA or WT rice. Serum samples from mice orally immunised with rice-expressed dmCT, CTB, dmCTA plus CTB or dmCTA or with WT rice or PBS, were subjected to GM1-ELISA. Binding of CT to the coated GM1 ganglioside was blocked in serum samples isolated from mice orally immunised with MucoRice-dmCT, -CTB or -dmCTA plus CTB but not MucoRice-dmCTA or WT rice or PBS (Fig. 5A). Furthermore, elongation assay revealed no morphological changes in CHO cells co-cultured with CT that had been pretreated with serum from mice orally vaccinated with MucoRice-dmCT or -CTB (Fig. 5B). In contrast, CT pretreated with serum from mice immunised with MucoRice-dmCTA or WT rice gave massive elongation of CHO cells